

## Confirmatory Appendices

### APPENDIX I: ANSI/ANS JET MODEL

#### I.1 INTRODUCTION

Debris generation is the first chronological step in the accident sequence for a postulated high-energy line break. In the idealized case of a double-ended guillotine break (DEGB), high-temperature, high-pressure reactor-cooling fluid may be ejected (from both sides of the broken pipe) that impinges on structures, equipment, piping, insulation, and coatings in the vicinity of the break. The degree of damage induced by the break jets is specific to the materials and structures involved, but the size and shape of the expanding jets and the forces imparted to surrounding objects depend on the thermodynamic conditions of the reactor at the location of the rupture. To maximize the volume of the damage zone, i.e., zone of influence (ZOI), it is conservative to consider free expansion of the break jet to ambient conditions with no perturbation, reflection, or truncation by adjacent structures. Spatial volumes of damage potential, as defined by empirical correlations of local jet pressure and observed damage, for example, can then be integrated over the free-jet conditions and remapped into convenient geometries, such as spheres or cones, that approximate the effects of congested reflection without crediting the associated shadowing, jet dispersion, and energy dissipation.

One reasonably accessible model that is available for computing pressure contours in an expanding jet is presented in Appendices B, C, and D of the American National Standards Institute (ANSI) guidance for the protection of nuclear power plants against the effects of pipe rupture [ANS88]. The ANSI model was used for the evaluation of potential damage volumes in the resolution of the boiling-water-reactor (BWR) strainer-blockage study [URG96, NRC98]. A similar approach suggested for this analysis by [ANS88] is a jet model developed at Sandia National Laboratories [WEI83]. Both the ANSI and the Sandia models were developed specifically for assessing structural loadings on relatively large targets near the jet centerline, so neither offers a true estimate of local pressures within a freely expanding jet. However, these models can be used with appropriate caution to learn a great deal about the spatial extent of and the thermodynamic conditions present within a high-energy jet.

This appendix presents the equation set needed to evaluate the ANSI model describing two-phase expansion of a jet from a broken high-energy line in a pressurized-water-reactor (PWR). To ensure a conservative review of the guidance report (GR), only the conditions related to full separation and full radial offset of a DEGB are developed. Alternative equations are presented in the standard for partial offsets and for longitudinal tears. This discussion is offered to resolve some of the confusion present in the notation of the standard and to provide a self-consistent basis for interpreting computational results relevant to PWR break conditions. The complexity of the jet model is somewhat beyond the scope of manual evaluation, but several investigators have performed successful spreadsheet calculations for discrete conditions. Routines developed in MATLAB and FORTRAN for evaluating the jet model are included at the end of this appendix as a further guide to implementation and for critical review; however, routines obtained from the National Institute of Standards and Technology (NIST) for evaluating thermodynamic state points are not provided.

## I.2 JET-MODEL FEATURES AND APPLICABILITY

Despite the apparent complexity of the equation set needed to evaluate the ANSI jet model, it is based on relatively few thermodynamic assumptions and limited comparisons with experimental observation. The bulk of the analytic detail supplies a geometric framework for interpolating jet pressures between assumed or observed transition points. Figure I-1 presents a sample calculation of jet pressure contours for a cold-leg DEGB. Although this calculation represents a relevant bound for evaluation of the GR, to be discussed later, the figure will be used first to introduce geometric features of the model.

The ANSI jet model subdivides the expanding jet into three zones that are delineated by dashed lines in Figure I-1. Zone 1 contains the core region, where it is assumed that liquid extrudes from the pipe under the same stagnation conditions as the upstream reservoir (interior red triangle). Zone 2 represents a zone of continued isentropic expansion, and Zone 3 represents a region of significant mixing with the environment, where the jet boundary is assumed to expand at a fixed, 10-degree, half angle. One group of equations from Appendix C of the standard defines the geometry of the jet envelope, and another group from Appendix D defines the behavior of internal pressure contours. Key geometry features that are determined by the thermodynamic conditions of the break include the length of the core region, the distance to the “asymptotic plane” between Zones 2 and 3, and the radii of the jet envelope at the transition planes between zones. At the asymptotic plane the centerline static pressure is assumed to approach the absolute ambient pressure outside of the jet.

Jet pressures provided by the ANSI model must be interpreted as local impingement gauge pressures. This is a property of the pressure field that is relevant to the interpretation of debris generation data; however, a subtle discrepancy exists between the ANSI model predictions and the desired local pressures. Because target materials may reside anywhere within the jet, fluid impingement can occur from a range of angles. Thus, idealized measurements or calculations of free-field impingement pressure should assume that the fluid stagnates (comes to rest) nonisentropically and parallel to the local flow direction. Note that a further subtlety appears here in the distinction between the classical definition of stagnation pressure that is related to the isentropic deceleration of flow along a streamline and the impingement pressure that includes entropy losses during impaction of a fluid on a physical test object. In general, impingement pressures will be higher than stagnation pressures, but the two terms may be used synonymously at times in this treatise.

In contrast to the desired local impingement pressure, the ANSI model appears to be concerned with total force loadings across relatively large objects placed near the jet centerline. It is stated in Appendix D of the standard that the pressure recovered on a target is related to the component of the flow perpendicular to the target and that, because of the diverging flow in an expanding jet, the pressure distribution on a large flat target will decrease in the radial direction. The pressure equations in the standard produce exactly this effect, and a brief allusion is made to a comparison of the predicted pressures with data taken across the face of large targets placed perpendicular to the jet. Further cautionary notes are given against applying the pressure equations to predict forces on small objects near the edges of the jet where flow velocities are clearly not parallel to the centerline.

These attributes of the model suggest that calculated pressures represent jet impingement conditions that would be experienced in a direction parallel to the midline only. Actual stream lines in a rapidly expanding jet must have a significant radial velocity component in order to create the characteristic envelope shown in Figure I-1, so in a sense, the predicted pressures represent only the longitudinal component of the local, momentum-dominated, total jet pressure. The implication of this interpretation is that true local impingement pressures as measured normal to realistic flow directions in the jet may be underestimated, particularly in Zones 1 and 2, where radial expansion is greatest.

Although a computed pressure isobar may be smaller in radius than that of the corresponding local impingement pressure that is desired for debris generation estimates, it may also be longer in the downstream direction. Comparative elongation of isobars from the jet model occurs because the entire mass flux ejected from the break is assumed to pass through the jet cross section at the asymptotic plane. Thus, the forward momentum of the jet is maximized in a manner that would be considered conservative for structural loading calculations. Unrealistic isobar elongation may also be predicted because the jet-centerline pressure equation for Zone 3 is inherently unbounded; that is, the centerline gauge pressure only falls to zero as the jet diameter grows infinitely large at infinite distance. It is impossible to quantify the net effect on isobar volume of these disparities between the ANSI model and the desired free-expansion impingement pressures without a complete understanding of the experimental measurements on which the model is based; however, the mathematical properties of the pressure equations are certain to exaggerate the length, and hence the volume, of low-pressure isobars.

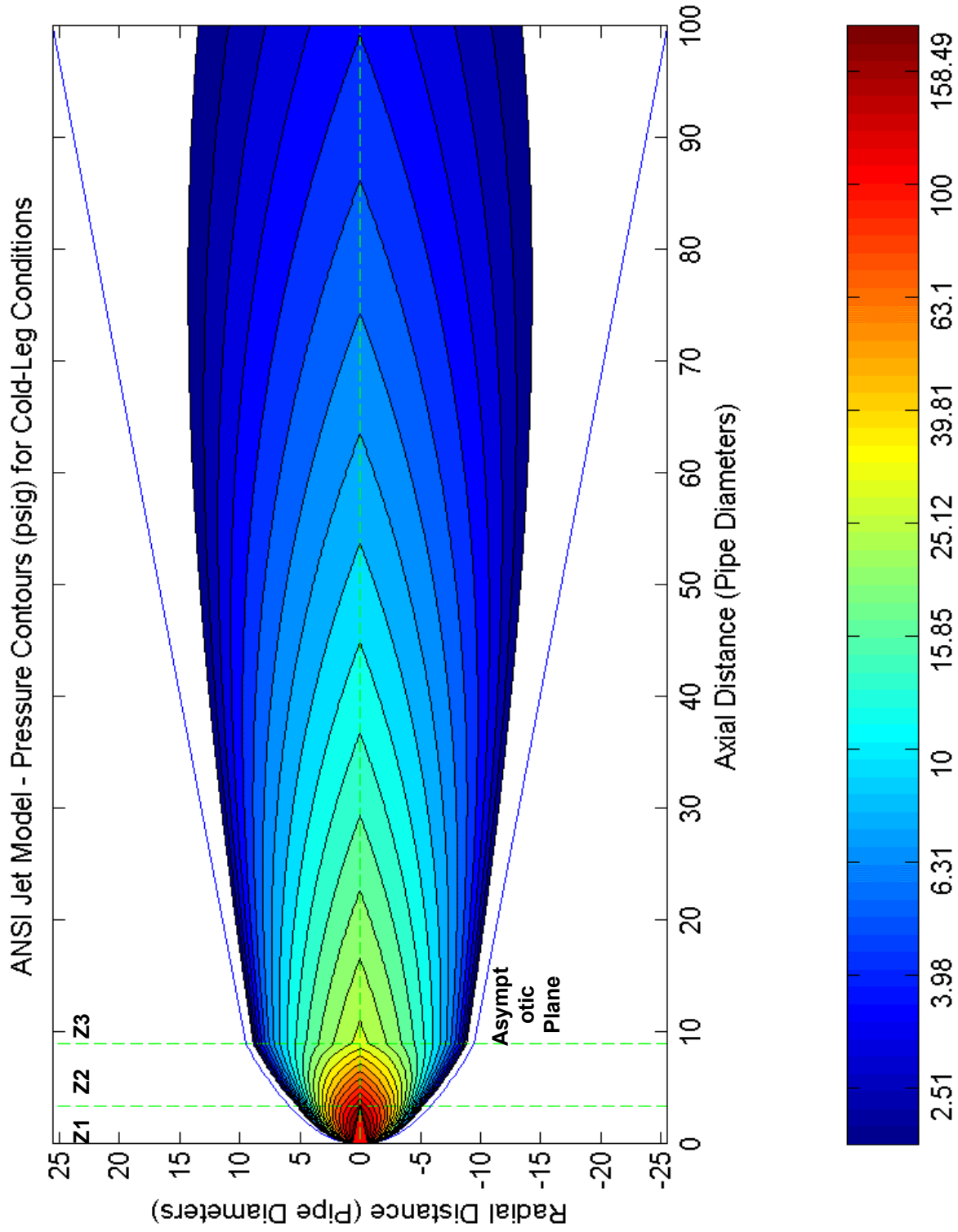


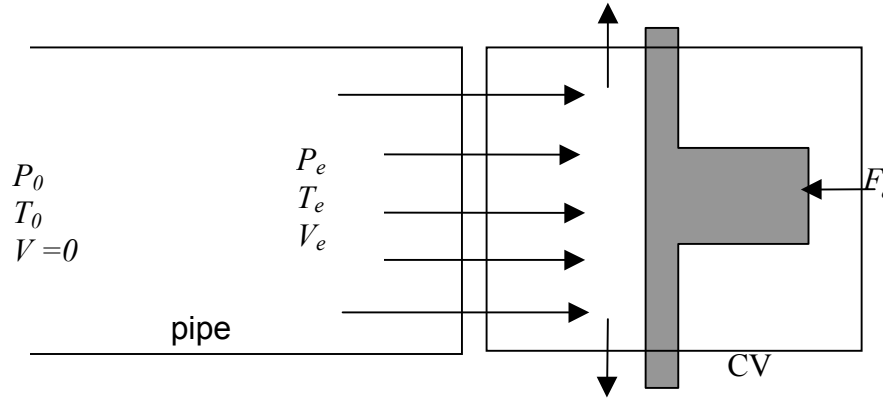
Figure I-1. ANSI Jet-Model Stagnation Pressures for PWR Cold-Leg Break Conditions (530°F, 2250 psia)

### I.3 JET-MODEL EQUATION SET

#### I.3.1 Fundamentals

Equations developed in the standard frequently refer to four distinct thermodynamic state points: (1) stagnation conditions of the fluid in the upstream reservoir denoted by subscript “0” (zero), (2) conditions at the exit plane of the pipe denoted by subscript “e”, (3) conditions at any point in the jet denoted either with subscript “j” or with no subscript at all, and (4) conditions at the asymptotic plane denoted by subscript “a”. These conventions are rigidly applied in the following development to resolve some notation inconsistencies found in the standard. Unless otherwise noted, pressures will refer to the absolute thermodynamic static pressure of the fluid. The first exception to this rule has already been mentioned—that is, the jet-pressure equations that define the local, gauge, longitudinal, impingement pressure.

**Figure I-2. Control-Volume Force Balance on a Rigid Plate near the Outlet**



One of the more fundamental relations in the model is actually presented near the end of the standard in Appendix D; it defines the total thrust (force) of the jet at the outlet. If a rigid plate were placed near the outlet, as shown in Figure I-2, the force balance on a control volume (CV) must consider both the static pressures and the rate of change of momentum acting on the boundary. If mass exits the control volume in a symmetric pattern at uniform velocity, the only possible force imbalance is in the x direction. The force on a plate near the exit is then

$$F_e = P_e A_e - P_{amb} A_e + \frac{1}{g_c} \frac{d}{dt} (m_e v_e) = (P_e - P_{amb}) A_e + \frac{1}{g_c} \left[ \left( \frac{d}{dt} m_e \right) v_e + m_e \left( \frac{d}{dt} v_e \right) \right], \quad (I-1)$$

where  $P_e$  is the fluid pressure at the exit plane,  $P_{amb}$  is the ambient pressure in containment,  $A_e$  is the area of the break, and  $m_e$  is the mass entering the control volume at velocity  $v_e$ . The force-to-mass conversion factor  $g_c$  equals 32.2 lbm·ft/lbf·s<sup>2</sup> in English units. Mass enters the control volume at constant velocity  $\left( \frac{d}{dt} v_e = 0 \right)$  at a rate

of  $\frac{d}{dt}m_e = \rho_e v_e A_e$ , where  $\rho_e$  is the fluid density at the exit. Thus, the total thrust generated at the exit plane is

$$F_e = (P_e - P_{amb})A_e + \frac{1}{g_c} \rho_e v_e^2 A_e. \quad \dots\dots\dots(1-2)$$

Substitution of  $G_e = \rho_e v_e$  for the critical mass flux crossing the exit plane yields

$$F_e = \left[ (P_e - P_{amb}) + \frac{G_e^2}{g_c \rho_e} \right] A_e, \quad \dots\dots\dots(1-3)$$

where the first term represents force applied by the static pressure of the fluid and the second term represents force imparted by the momentum of the fluid. The ambient pressure is often assumed to be zero to maximize the available jet thrust conservatively.

Division of Equation (1-2) or (1-3) by the exit area suggests an effective, or area-averaged, jet pressure of  $\bar{P}_e = F_e/A_e$ . This effective pressure will be greater than the classical stagnation pressure at the exit, which is defined by Bernoulli's equation as

$$P_e^{stag} = P_e^{static} + \frac{1}{2g_c} \rho_e v_e^2, \text{ because the derivation of Bernoulli's law requires that the fluid}$$

be brought to rest in an idealized, reversible manner. Jet impingement on a body is a highly anisentropic process. For an incompressible fluid, the static pressure at the exit equals the ambient pressure, and if friction losses in piping between the reservoir and the break can be neglected, the stagnation pressure at the exit equals the initial pressure. Under these conditions, Bernoulli's equation can be written as

$$\frac{1}{g_c} \rho_e v_e^2 = 2(P_0 - P_{amb}). \quad \dots\dots\dots (1-4)$$

Equations (1-2) and (1-3) are often simplified as  $F_e = C_T P_0 A_e$ , where  $P_0$  is the upstream stagnation pressure and  $C_T$  is the thrust coefficient defined by comparison to be

$$C_T = \frac{1}{P_0} \left[ \frac{1}{g_c} \rho_e v_e^2 + (P_e - P_{amb}) \right] = \frac{1}{P_0} \left[ \frac{G_e^2}{g_c \rho_e} + (P_e - P_{amb}) \right]. \quad \dots\dots\dots(1-5)$$

Equation (1-5) emphasizes that the correlation between upstream stagnation pressure and the thrust coefficient is determined by the fluid properties that exist at the exit plane. Several alternative models are available to describe the thermodynamic transitions occurring in a high-energy fluid that is expanding and accelerating, which, in turn, determine the exit density, and the critical mass flux. It is very important that the specification of  $C_T$  be consistent with the models used to evaluate  $G_e$  and  $\rho_e$ . It should be noted that the standard uses inconsistent notation for the thrust coefficient (ex.

$C_T, C_{T_e}, C_{T_e}^*$ ). All forms must refer to a single numeric value if the pressure equations are to be piecewise continuous between jet zones.

Under the conditions of zero friction loss and incompressible flow (solid liquid with no vapor fraction where  $P_e = P_{amb}$ ), Equation (I-4) can be substituted into Equation (I-5) to obtain a theoretical maximum value of  $C_T = 2.0$  when ambient pressure is neglected. By treating steam as a perfect gas under isentropic flow to obtain the exit velocity, Shapiro [SHA53] derives a lower theoretical limit of  $C_T = 1.26$ . Any numeric evaluation of Equation (I-5) using water property tables to derive  $G_e$  and  $\rho_e$  should be compared to these limits. Although it is clearly most conservative to apply the liquid limit for all state points, numerical evaluation of Equation (I-5) using water tables is sufficiently robust to permit this refinement. Recommendations for computing the thrust coefficient are discussed in Section I.4 later in this appendix, and convenient reference figures are provided.

### I.3.2 Jet-Envelope Geometry

The shape and size of the jet envelope predicted by the ANSI model are dictated by the thermodynamic conditions upstream of the break. Except where noted, spatial distances are represented in dimensionless multiples of the broken-pipe inside diameter,  $D_e$ . Jet boundaries (and pressure contours) can be scaled in this manner because the equation set is linear with respect to pipe diameter. Linearity can be proven rigorously by factoring and eliminating terms of  $D_e$  in every equation. In general, because of potential nonlinearities, it is not sufficient to evaluate a complicated dimensional equation set at a unit value of a candidate scaling parameter and then to assume that the unit result can be multiplied by any desired value of that parameter. To recover physical quantities for a particular pipe size, dimensionless distances must be multiplied by  $D_e$ , dimensionless areas must be multiplied by  $D_e^2$ , etc.

The distance of extrusion by the jet core is

$$L_c = 0.26\sqrt{\Delta T_{sub}} + 0.5 \quad , \quad \dots\dots\dots(I-6)$$

where  $\Delta T_{sub}$  is the degree of subcooling (°F) upstream of the break location, i.e., the difference between the saturation temperature  $T_{sat}$  at the system pressure  $P_0$  and the system temperature  $T_0$ . The jet core is shown by the interior red triangle in Figure I-1. Note that  $L_c$  takes on a value of 0.5 for saturated or superheated conditions. Also, if  $L_c > L_a$ , the distance to the asymptotic plane defined below,  $L_c$  should be set to zero and the jet pressure should be assumed to be uniform across the break area at a value of  $\bar{P}_j = (F_e / A_e) / C_T$ , where the ratio  $F_e / A_e$  is computed from Equation (I-2) or (I-3). This can occur for low-pressure nonexpanding jets. A jet can be treated as nonexpanding when the initial temperature of a liquid reservoir is less than the

saturation temperature at  $P_{amb}$  or the initial pressure of a gas reservoir is equal to ambient pressure,  $P_0 = P_{amb}$ .

The diameter of the jet at the exit plane is defined to be

$$D_{je} = \sqrt{C_T}, \quad \dots\dots\dots(1-7)$$

which is slightly larger than the diameter of the pipe because  $1.26 \leq C_T \leq 2.0$ .

The diameter of the jet at the asymptotic plane (Zone 2 to Zone 3 boundary) is defined by the relation

$$D_a^2 = \frac{G_e^2}{g_c \rho_a C_T P_0}, \quad \dots\dots\dots(1-8)$$

where  $\rho_a$  is the homogeneous fluid density at the centerline distance to this plane, which is given by

$$L_a = \frac{1}{2}(D_a - 1). \quad \dots\dots\dots(1-9)$$

Note that some care must be taken to keep pressure and mass flux dimensionally consistent in Equation (1-8). The density  $\rho_a$  is to be evaluated at a state point defined by the system enthalpy  $h_o$  and an asymptotic-plane static pressure defined by

$$P_a = \left\{ 1 - 0.5 \left( 1 - \frac{2P_{amb}}{P_o} \right) f(h_o) \right\} P_{amb}, \quad \dots\dots\dots(1-10)$$

where

$$f(h_o) = \sqrt{0.1 + \frac{h_o - h_f}{h_{fg}}} \text{ for } \frac{h_o - h_f}{h_{fg}} > -0.1, \text{ and } f(h_o) = 0 \text{ otherwise.} \quad (1-11)$$

Within the condition stated by Equation (1-11),  $h_f$  and  $h_g$  are the saturated fluid enthalpy and saturated vapor enthalpy at  $P_0$ , respectively, and  $h_{fg} = h_g - h_f$  is the heat of vaporization. Further conditions on Equation (1-10) are that if the ratio  $P_{amb} / P_0 > 1/2$ , it should be set equal to 1/2 and that, as a static pressure,  $P_a \geq 0$ .

The first criterion on  $f(h_o)$  simply checks whether the initial quality  $x_0 = \frac{h_o - h_f}{h_{fg}}$  is greater than negative 10%. When considered as a whole, these conditions imply that

$0 \leq P_a \leq P_{amb}$ . If the initial fluid is more than 10% subcooled, the jet static pressure equals ambient pressure at the asymptotic plane. If the jet is less than 10% subcooled, the jet static pressure at the asymptotic plane can be lower than ambient pressure. Equation (I-10) suggests that the asymptotic plane is placed at the distance where the jet static pressure approaches ambient pressure. The distance to this plane given by Equation (I-9) may simply have been chosen by geometric comparison with observed jets.

The state point defined by the asymptotic pressure  $P_a$  and the system enthalpy  $h_0$  may be a two-phase condition. In this case, it is necessary to evaluate the asymptotic density

$\rho_a$  using the quality  $x_a = \frac{h_o - h_{fa}}{h_{ga} - h_{fa}}$ , where  $h_{fa}$  and  $h_{ga}$  are the saturated fluid and

vapor enthalpies at  $P_a$ , respectively. Then  $\rho_a = \left[ \frac{x_a}{\rho_{ga}} + \frac{1-x_a}{\rho_{fa}} \right]^{-1}$ , where  $\rho_{fa}$  and  $\rho_{ga}$

are the saturated fluid and vapor densities at  $P_a$ , respectively. Automated steam tables generally give mixture densities directly for a two-phase state point, so this complication may be unnecessary.

The similarity of terms in Equation (I-8) to the force-balance equations derived in the previous section suggests a different interpretation for the asymptotic plane. For convenient reference, the jet diameter at the asymptotic plane is again given by

$$D_a^2 = \frac{G_e^2}{g_c \rho_a C_T P_0}, \quad \dots\dots\dots(I-12)$$

Given the discussion following Equation (I-3) and the definition of the thrust coefficient, the factors  $C_T P_0$  in Equation (I-12) are immediately recognized as  $\bar{P}_e = F_e / A_e$ , the average total jet pressure at the exit. If a relation similar to Equation (I-3) is written to describe the area-averaged pressure across the jet cross section at the asymptotic plane,

$$\bar{P}_a = \frac{F_a}{A_a} = \left[ (P_a - P_{amb}) + \frac{G_e^2}{g_c \rho_a} \right], \quad \dots\dots\dots(I-13)$$

then the term  $G_e^2 / g_c \rho_a$  in Equation (I-12) is recognized to be  $\bar{P}_a - (P_a - P_{amb})$ . If the static pressure at the asymptotic plane  $P_a$  is not much different than the ambient pressure  $P_{amb}$ , then Equation (I-12) reduces to the ratio of average pressures computed over the jet cross section at the asymptotic plane and over the jet cross section at the exit,

$$D_a^2 = \frac{F_a / A_a}{F_e / A_e} = \frac{\bar{P}_a}{\bar{P}_e}. \quad \dots\dots\dots(I-14)$$

Writing explicitly the definition of the dimensionless asymptotic-plane area as  $D_a^2 = \frac{A_a}{A_e}$

illustrates that the diameter of the jet given by Equation (I-8) has been chosen at the point where the ratio of average pressures approaches the ratio of cross sectional areas, and for this to be true, the total force across each area must be the same. Hence, the ANSI model implicitly assumes that the jet force available at the outlet is conserved across the jet cross section at the asymptotic plane. At this distance, the jet is presumed to begin interacting with the environment. This development also shows that the ANSI model projects the entire mass flux across the asymptotic plane rather than following more realistic stream lines across the jet boundary in Zones 1 and 2. Equation (I-8) is derived more rigorously in Section I-4 to further emphasize these points.

The remainder of the jet envelope is simply interpolated as a function of centerline distance  $L$  between the transition diameters discussed above. Within Zone 1, the diameter of the jet core is given by

$$D_c = \sqrt{C_T} \left( 1 - \frac{L}{L_c} \right) \quad \dots\dots\dots(I-15)$$

For Zone 1 and 2 ( $0 < L \leq L_a$ ), the jet diameter is given by

$$D_j^2 = \left[ 1 + \frac{L}{L_a} \left( \frac{D_a^2}{D_{je}^2} - 1 \right) \right] D_{je}^2 \quad \dots\dots\dots(I-16)$$

In Zone 3 ( $L > L_a$ ), the jet diameter expands at a 10-degree half angle beginning from the diameter at the asymptotic plane. The Zone-3 diameter is specified by

$$D_j^2 = \left[ 1 + \frac{2(L - L_a)}{D_a} \tan(10^\circ) \right]^2 D_a^2 \quad \dots\dots\dots(I-17)$$

### I.3.3 Jet Pressures

Pressure contours also appear to be interpolated from a limited number of geometric reference points, but the basis for this interpolation is not evident from the standard. It can be shown that all equations are piecewise continuous at the separation planes between zones; however, no effort was made to match first-derivative slopes. This deficiency admits the possibility of “kinks” in the contours, as observed in Figure I-1 across the boundary between Zones 2 and 3. Pressure contours in Zone 1 ( $0 \leq L \leq L_c$ ) depend on the following discriminant. If

---

\* This observation was derived from the jet equations and is not expounded as part of any derivation in the standard. It is simply an implication of the definitions.

$$D_j^2 + 2D_j D_c + 3D_c^2 \leq 6C_T, \quad \dots\dots\dots(I-18)$$

then the jet pressures are given as a function of radius ( $r_c < r \leq r_j$ ) for jet diameters  $D_j = 2r_j$  as

$$P_j = \left( \frac{D_j - 2r}{D_j - D_c} \right) \left[ 1 - \frac{2(D_j^2 + D_j D_c + D_c^2 - 3C_T)}{D_j^2 - D_c^2} \left( \frac{2r - D_c}{D_j - D_c} \right) \right] P_0. \quad \dots\dots\dots(I-19)$$

Otherwise,

$$P_j = \left( \frac{D_j - 2r}{D_j - D_c} \right)^2 \left[ \frac{6(C_T - D_c^2)}{(D_j - D_c)(D_j + 3D_c)} \right] P_0. \quad \dots\dots\dots(I-20)$$

It is important to note that the leading term ( $D_j - 2r$ ) vanishes in both Equation (I-19) and (I-20) as the radius approaches the jet envelope where the absolute pressure equals  $P_{amb}$ . Therefore, evaluations of  $P_j$  must be interpreted as gauge pressures. In

Equation (I-19), the term  $\left( \frac{2r - D_c}{D_j - D_c} \right)$  ensures that the jet pressure matches  $P_0$  on the boundary of the core. There is no similar constraint provided in Equation (I-20), so there will be a sharp discontinuity in pressure at the boundary of the jet core when this condition is invoked, as shown in Figure I-1. Equations (I-19) and (I-20) were not intended to be evaluated inside of the core region. Within the core, the system stagnation conditions are presumed to hold.

In Zones 2 and 3, jet pressures are parameterized in terms of the jet centerline pressure  $P_{jc}$ . In Zone 2 ( $L_c < L \leq L_a$ ),

$$P_{jc} = \left\{ F_c - \left( F_c - \frac{3C_T}{D_a^2} \right) \frac{L_a}{L} \frac{(L - L_c)}{(L_a - L_c)} \right\} P_0, \quad \dots\dots\dots(I-21)$$

where the parameter  $F_c = 1.0$  if  $D_j^2 \leq 6C_T$  at distance  $L_c$  and  $F_c = 6C_T / D_j^2$  otherwise. When  $L = L_c$ , Equation (I-21) reduces to  $P_{jc} = F_c P_0$ . If  $F_c = 1.0$ , the centerline pressure will match the assumed pressure in the core region, but otherwise, there will again be a discontinuity. Given the centerline pressure, jet pressures in Zone 2 are specified by

$$P_j = \left( 1 - \frac{2r}{D_j} \right) \left\{ 1 - 2 \left( \frac{2r}{D_j} \right) \left[ 1 - \frac{3C_T}{D_j^2} \frac{P_0}{P_{jc}} \right] \right\} P_{jc}. \quad \dots\dots\dots(I-22)$$

It can be shown by integration that (I-22) is essentially a geometric rather than physical condition: it leads to full recovery of the jet force anywhere in Zone 2 regardless of the value assigned to the jet diameter. In Zone 3, centerline pressures are given by

$$P_{jc} = \frac{3C_T P_0}{D_a^2 \left[ 1 + \frac{2(L - L_a)}{D_a} \tan(10^\circ) \right]^2} \dots\dots\dots(I-23)$$

and jet pressures are given by

$$P_j = \left( \frac{D_j - 2r}{D_j} \right) P_{jc} \dots\dots\dots(I-24)$$

Pressures on the transition between Zones 2 and 3 are piecewise continuous, including on the centerline.

### I.3.4 Pressure-Contour Characteristic Equations

Equations presented in the previous section can be used to evaluate longitudinal impingement pressures at any location in the jet. However, in the present forms, they are not particularly convenient for identifying geometric characteristics such as isobar boundaries. Similarly, when numerically computing volumes under a given isobar, it is convenient to know the downstream range of the contour, which always begins at  $L = 0$  and terminates in a cusp on the centerline at some distance  $L = L_t(P_j)$ . Relationships presented in this section are not developed in the ANSI standard; they are offered to facilitate some of the many practical details involved with implementing the standard.

Figure I-1 illustrates the typical behavior of jet-pressure isobars generated by the ANSI model. The isobars outlined in black represent lines of constant pressure that can be found by solving the pressure Equations (I-19), (I-20), (I-22), and (I-24) for the radii at a constant pressure  $P_j$ . Remember that the downstream distance  $L$  is implicitly specified by the jet diameter  $D_j$ . Each pressure equation can be reduced to a general quadratic expression for the radius of the form  $Ar^2 + Br + C = 0$ .

The coefficients from Equation (I-19) for Zone 1 are

$$A = 4H, \quad B = -2[1 + H(D_j + D_c)], \quad \text{and} \quad C = D_j + HD_j D_c + (D_c - D_j) \frac{P_j}{P_0}, \dots\dots\dots(I-25)$$

where

$$H = 2 \frac{(D_j^2 + D_j D_c + D_c^2 - 3C_T)}{(D_j^2 - D_c^2)(D_j - D_c)} \dots\dots\dots(I-26)$$

The coefficients from Equation (I-20) for Zone 1 are

$$A = 4, \quad B = -4D_j, \quad \text{and} \quad C = D_j^2 - (D_j - D_c)^2 \frac{P_j}{P_0} I, \quad \dots\dots\dots(I-27)$$

where

$$I = \frac{6(C_T - D_c^2)}{(D_j - D_c)(D_j + 3D_c)}. \quad \dots\dots\dots(I-28)$$

A special case occurs in Zone 1 at  $L = 0$ , where  $D_j = D_c$  and  $r = D_j/2 = D_c/2$  for all  $P_j$ .

Equation (I-22) yields the following coefficients for Zone 2:

$$A = 8 \frac{J}{D_j^2}, \quad B = -\left(\frac{2}{D_j} + \frac{4J}{D_j}\right), \quad \text{and} \quad C = 1 - \frac{P_j}{P_{jc}}, \quad \text{where} \quad J = \left(1 - \frac{3C_T}{D_j^2} \frac{P_0}{P_{jc}}\right). \quad \dots\dots\dots(I-29)$$

Finally, Equation (I-24) yields for Zone 3 the coefficients

$$A = 0, \quad B = -2/D_j, \quad \text{and} \quad C = 1 - \frac{P_j}{P_{jc}}. \quad \dots\dots\dots(I-30)$$

The analytic solution for radius in Zone 3 is

$$r = \frac{1}{2} D_j \left(1 - \frac{P_j}{P_{jc}}\right). \quad \dots\dots\dots(I-31)$$

The sharp tip of each contour shown in Figure I-1 is another nonphysical feature of the ANSI model that arises from lack of attention to matching spatial first derivatives. It might be expected that each isobar be smoothly bounded and have infinite slope at the terminal point, especially at very low pressures where the jet returns to ambient conditions. It is helpful to know the distance to the terminal point of each contour for iterative integration of spatial volumes. These points can be found by solving the centerline pressure Equations (I-21) and (I-23) for distances  $L_t$  corresponding to the desired pressure. Note that there are no terminal points in Zone 1 except for the jet core.

For Zone 2 from Equation (I-21) comes the relation

$$L_t = \frac{L_c}{1 - \frac{L_a - L_c}{RL_a} \left( F_c - \frac{P_j}{P_0} \right)}, \quad \dots\dots\dots(I-32)$$

where

$$R = F_c - \frac{3C_T}{D_a^2}, \quad \dots\dots\dots(I-33)$$

and for Zone 3 from Equation (I-23) comes the relation

$$L_t = \frac{1}{2} \left[ \left( \frac{3C_T P_0}{D_a^2 P_j} \right)^{1/2} - 1 \right] \frac{D_a}{\tan(10^\circ)} + L_a. \quad \dots\dots\dots(I-34)$$

One remaining practicality is the numerical integration of pressure isobars defined by Equations (25), (27), (29), and (31). If these equations are evaluated at a set of discrete distances  $L_i$ , the corresponding radii  $r_i$  define adjacent conical frusta with unique slopes as shown in Figure I-3. The analytic formula for the frustum of a cone is given by

$$V_i = \pi \left[ \frac{1}{3} m^2 L^3 + m_i (r_{i+1} - m_i L_{i+1}) L^2 + (m_i^2 L_{i+1}^2 - 2r_{i+1} m_i L_{i+1} + r_{i+1}^2) L \right]_{L_i}^{L_{i+1}} \quad \dots\dots\dots(I-35)$$

where the linear slope of the sides of the conical segment  $m = \frac{r_{i+1} - r_i}{L_{i+1} - L_i}$ . The total volume under the isobar is approximated by the sum  $V_{isobar} = \sum V_i$  and can be refined to any desired accuracy by evaluating the pressure-isobar equations at finer resolution.

The total volume of an isobar should be multiplied by a factor of 2 when double-ended breaks of equivalent upstream pressure are being considered, and finally, converted to a volume-equivalent sphere by the formula

$$R_{sphere} = \left( \frac{3}{4\pi} V_{isobar} \right)^{1/3}. \quad \dots\dots\dots(I-36)$$

#### I.4 DERIVATION OF ASYMPTOTIC-PLANE AREA

To obtain Equation (I-8) for the jet diameter  $D_a$  at the asymptotic plane, force balances are applied to the two control volumes shown in Figure I-4 in a manner analogous to the derivation of the thrust force given by Equation (I-2). In the figure, a plate is positioned normal to the flow at the asymptotic plane. The force required to hold the plate in static equilibrium is notated  $F_e$ . The fluid deflected by the plate is assumed to exit the control

volume isotropically in a plane oriented parallel to the face of the plate. Exit flow is not represented in the figure.

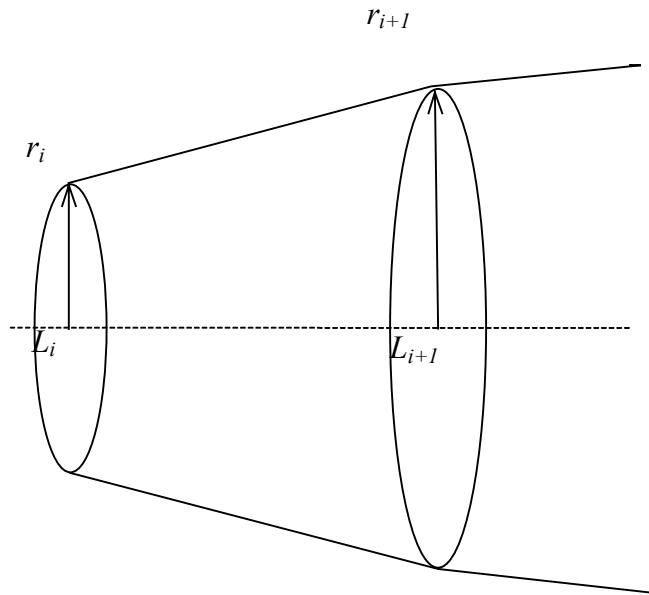


**Figure I-3. Linear Segmentation of Jet Cross Sections for Numerical Volume Integration**

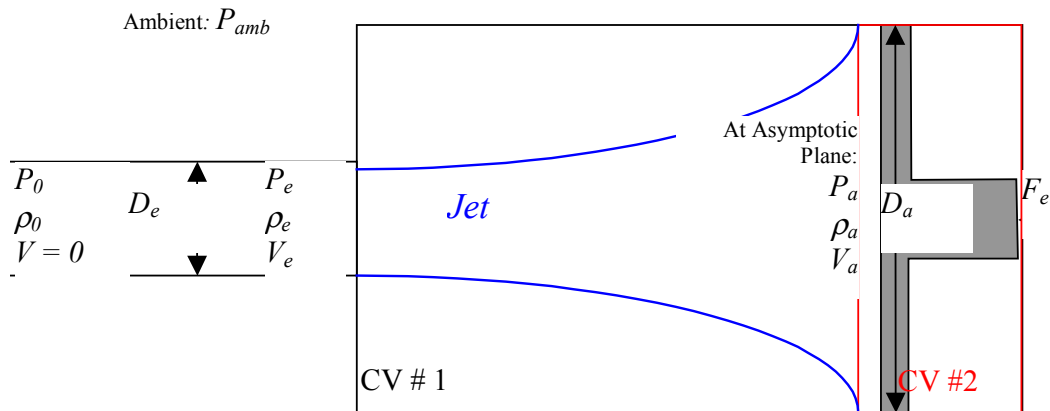


**Figure I-4. Control-Volume Force Balances on a Rigid Plate at the Asymptotic Plane**

It is assumed in Appendix C of the standard (p. 52) that the fluid does not begin to interact with the surrounding environment until after it crosses the asymptotic plane. Hence, no energy is supplied to or removed from the jet in the region described by the two control volumes in Figure (I-4). Therefore, the entire jet force is recovered, and the force balance for CV #1 is identical to that given by Equation (I-1).

The jet characteristics at the asymptotic plane – fluid density  $\rho_a$ , velocity  $v_a$ , and static pressure  $P_a$  – are not expected to be uniform, so to render the force balance for CV #2 tractable, these properties are assumed to be averaged over the jet cross section. The force balance in the direction of the jet flow for control volume #2 may hence be written as

$$F_e = (P_a - P_{amb})A_a + \frac{1}{g_c} \left( v_a \frac{d}{dt} m_a + m_a \frac{d}{dt} v_a \right), \quad \dots\dots\dots(I-37)$$

where  $A_a = \pi D_a^2 / 4$  is the jet area at the asymptotic plane and  $m_a$  is the mass of the fluid located within the control volume.

For steady flow,  $dv_a/dt = 0$ . The rate at which mass enters the control volume,  $dm_a/dt$ , is simply the total mass flow crossing the asymptotic plane and is given by

$$\frac{dm_a}{dt} = \rho_a v_a A_a. \quad \dots\dots\dots(I-38)$$

Hence, the force balance simplifies to

$$F_e = (P_a - P_{amb})A_a + \frac{1}{g_c} \rho_a v_a^2 A_a. \quad \dots\dots\dots(I-39)$$

Since no mass escapes the jet between the break location and the asymptotic plane, the mass flow rates at the break and at the asymptotic plane must be equal, i.e.,

$$\rho_a v_a A_a = \rho_e v_e A_e. \quad \dots\dots\dots(I-40)$$

This relation may be employed to eliminate  $v_a$  in the force balance.

As mentioned in the discussion following Equation (I-11), the static pressure at the asymptotic plane is generally taken to be equal to  $P_{amb}$ . Setting  $P_a$  equal to  $P_{amb}$  yields

$$F_e = \frac{1}{g_c} \frac{\rho_e^2 v_e^2 A_e^2}{\rho_a A_a}. \quad \dots\dots\dots(I-41)$$

Setting this evaluation of  $F_e$  equal to that obtained from the force balance on CV #1, Equation (I-2), gives the result

$$\frac{A_a}{A_e} = \frac{\rho_e^2 v_e^2}{g_c \rho_a} \cdot \frac{1}{(P_e - P_{amb}) + \frac{1}{g_c} \rho_e v_e^2} \quad \dots\dots\dots(I-42)$$

The second fraction in this equation is recognized by comparison with Equation (I-5) as being equal to  $1/(C_T P_0)$ . Making use of the mass flux definition  $G_e = \rho_e v_e$ , leads to the expression for the jet area at the asymptotic plane given in the standard,

$$\frac{A_a}{A_e} = \frac{G_e^2}{g_c \rho_a C_T P_0} \quad \dots\dots\dots(I-43)$$

The standard recommends that the density  $\rho_a$  at the asymptotic plane be evaluated using the local static pressure  $P_a$  and the system stagnation enthalpy  $h_0$  rather than the local static enthalpy  $h_a$ . Therefore, it is implicitly assumed that the dynamic enthalpy at the asymptotic plane,  $v_a^2/2$ , is small.

An inconsistency is noted here because  $P_a$  in the ANSI jet model – as governed by equation (I-10) – is not always equal to  $P_{amb}$ , yet the asymptotic plane area is always computed as if this were the case. For slightly subcooled, saturated, or two-phase upstream conditions, application of Equation (I-10) leads to a value for  $P_a$  that is less than  $P_{amb}$ . Although the physical reasoning behind Equation (I-10) is not documented in the standard, it appears to correct for cases in which the dynamic enthalpy is non-negligible. This development further confirms that only longitudinal pressures are being computed for  $P_{jet}$ , at least at the asymptotic plane, and probably everywhere within the jet envelope.

## I.5 CRITICAL FLOW MODELS

### I.5.1 Discharge Mass Flux

Results produced by the jet model are sensitive to the value assigned to the mass flux discharged from the break plane,  $G_e$  [lbm/ft<sup>2</sup>/s]. The area of the jet at the asymptotic plane  $A_a$  [ft<sup>2</sup>], i.e., the cross sectional area reached by the jet following free (isentropic) expansion, is proportional to  $G_e^2$ . Thus,  $G_e$  is indirectly specified via Figures C-4 and C-5 in the standard, which plot the ratio of the asymptotic area to the break plane area  $A_a/A_e$  for upstream conditions ranging from 50°F subcooled liquid to saturated vapor. Aside from difficulties inherent in recovering numerical values from coarsely resolved plots, use of these figures is not recommended for two reasons:

1. The range of upstream stagnation conditions covered by the plot – extending only to 50oF subcooling – is insufficient. Typical cold-leg conditions in a PWR might entail subcooling of 100oF or more.
2. The origin of the results is unclear. Which model was used to evaluate the relevant mass fluxes and thrust coefficients? Without this information, there can be no confidence that the rest of the model will be applied in a self-consistent manner.

Therefore, we strongly concur with the recommendation given in the standard (p. 57) that a two-phase critical flow model be employed to evaluate  $G_e$ . Two models that are in widespread use are cited: the homogeneous equilibrium model (HEM)<sup>†</sup> and the Henry-Fauske model [HEN71]. The standard provides a loose recommendation regarding the applicability of the models as a function of upstream stagnation properties: the HEM for saturated or two-phase and Henry-Fauske for subcooled conditions.

Several pitfalls await a naïve application of this guidance. To facilitate the exposition of these pitfalls, it is useful first to provide a simplified description of the physics inherent in each of the models.

Under the HEM, the phases are assumed to be in thermodynamic equilibrium and to remain well mixed. The relative velocity between the phases is therefore assumed to be zero. External heat transfer, wall roughness, and other interactions with the environment are neglected so that the expansion is isentropic.

Given these assumptions, the first law of thermodynamics is applied to the homogenized fluid. Combined with the definition of the mass flux, the first law yields an expression for  $G_e$  in terms of the mixture's static properties at the choked point. The critical mass flux is defined as the value of  $G_e$  that maximizes this expression. Numerical solution of the HEM is thus an iterative process, entailing a search over the space of static state points that preserve the upstream stagnation entropy.

The Henry-Fauske model preserves some of the assumptions made under the HEM, namely that the mass flux may be expressed as a function of the thermodynamic state at the throat, that the critical mass flux can be obtained by maximizing this function, and that the expansion is isentropic. However, Henry and Fauske argue that the assumptions of homogeneous mixing and thermodynamic equilibrium during the expansion are unrealistic given the short time scales involved. Rather, interphase mass transfer is constrained such that the quality  $x_t$  at the throat is equal to the upstream stagnation quality  $x_0$ . Heat transfer during the expansion is also assumed negligible; the liquid-phase temperature  $T_{ft}$  at the throat is held fixed at the upstream liquid temperature  $T_{f0}$ . The temperature of the vapor phase, if it is present, is allowed to vary. The heat- and mass-transfer rates at the throat are treated as significant, and expressions for these are developed assuming polytropic vapor behavior.

---

<sup>†</sup> For a discussion of practical considerations surrounding implementation of the HEM, as well as a tabulation of results for a wide range of upstream conditions, see Ref. [HAL80].

In practice, the Henry-Fauske model is implemented by solving a transcendental equation for the static pressure at the throat that maximizes mass flux. Both Henry-Fauske and the HEM are evaluated through iterative procedures, with thermodynamic properties being queried upon each iteration. Therefore, the models were coded as a series of FORTRAN subroutines, driven by a MATLAB control function, that directly couple with the FORTRAN implementation of the NIST/American Society of Mechanical Engineers (ASME) steam tables [HAR96] when fluid properties are required. The results obtained from the software were successfully validated against those presented in Refs. [Hal80] and [Hen71]. These programmed routines allow a thorough assessment of the practical ramifications of using each model within the ANSI jet-modeling framework.

The standard does not provide guidance with regard to critical flow modeling for superheated conditions. The simplest approach would be to treat the steam as an ideal gas and apply the appropriate equation of state. This treatment was attempted and found to be highly inadvisable for the slightly superheated states that are of most relevance to the present application. Two qualitative observations support this conclusion: first, when the upstream superheat is small the flow at the choked location is in fact two phase; second, slightly superheated high-pressure steam does not exhibit the typically assumed idealized properties (e.g., a specific heat ratio of 1.3) so that transitions evaluated using the ideal gas law would not preserve entropy. These considerations lead us to recommend that the HEM be used to treat the superheated state points that may arise in this application.

As mentioned above, the standard does provide guidance for two-phase and single-phase liquid stagnation state points. Specifically, it recommends the use of HEM for saturated and Henry-Fauske for subcooled upstream conditions. We believe that the Henry-Fauske model should, in fact, be employed for both of these regimes. This recommendation stems from several considerations, as outlined below.

Critical mass fluxes predicted by the HEM and Henry-Fauske models exhibit their most significant disagreement at precisely the transition point recommended in the standard, i.e., for saturated-liquid upstream conditions. Figure I-5 and Figure I-6 provide contour plots of  $G_e$  as obtained from the two models for subcooled vessel stagnation conditions. In figures showing flow properties for subcooled state points, the stagnation temperature is varied on the x axis and pressure on the y axis. The regions between contour lines of constant  $G_e$  are shaded for ease of delineation. Because the domain of validity of the flow models does not extend to superheated conditions, pressure and temperature combinations that lie within this regime are blanked out on the plots. Mass fluxes for saturated upstream conditions are shown in Figure I-7 and Figure I-8. In these plots,  $G_e$  is calculated at several saturated (temperature, pressure) state points as a function of the vessel quality.

Figure I-9 and Figure I-10 display the variation between the HEM and Henry-Fauske mass fluxes. It can be seen from these figures that discrepancies of 50% or more exist for saturated liquid upstream conditions and that significant variations persist for slightly subcooled and low-quality two-phase stagnation conditions. This disagreement follows from a variation in the assumptions regarding interphase mass transfer. Because the quality is held fixed under the Henry-Fauske model, the discharge is almost entirely in the liquid phase. Under the HEM, however, heat and mass transfer between the phases

is allowed and the discharge has a quality that is significantly greater than zero. This discharge possesses a lower density and higher velocity than that predicted by Henry-Fauske. It can be shown numerically that the HEM mass flux prediction will be lower than that of Henry-Fauske for the slightly subcooled, saturated liquid, and low-quality upstream conditions in which the HEM prediction of discharge quality is markedly higher than that of Henry-Fauske.

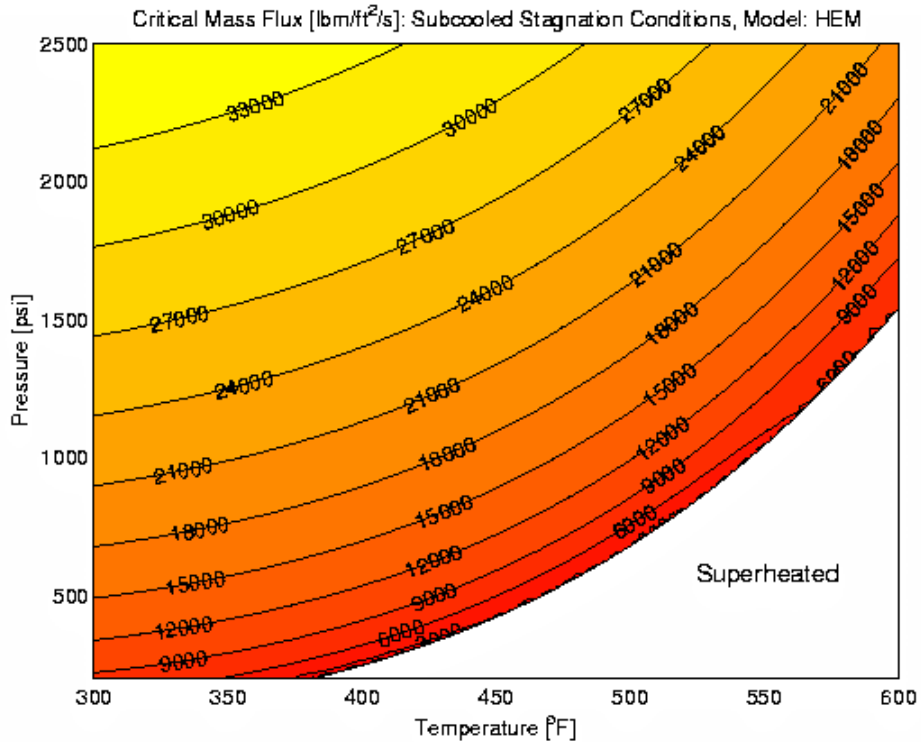


Figure I-5. HEM Critical Mass Flux, Subcooled Stagnation

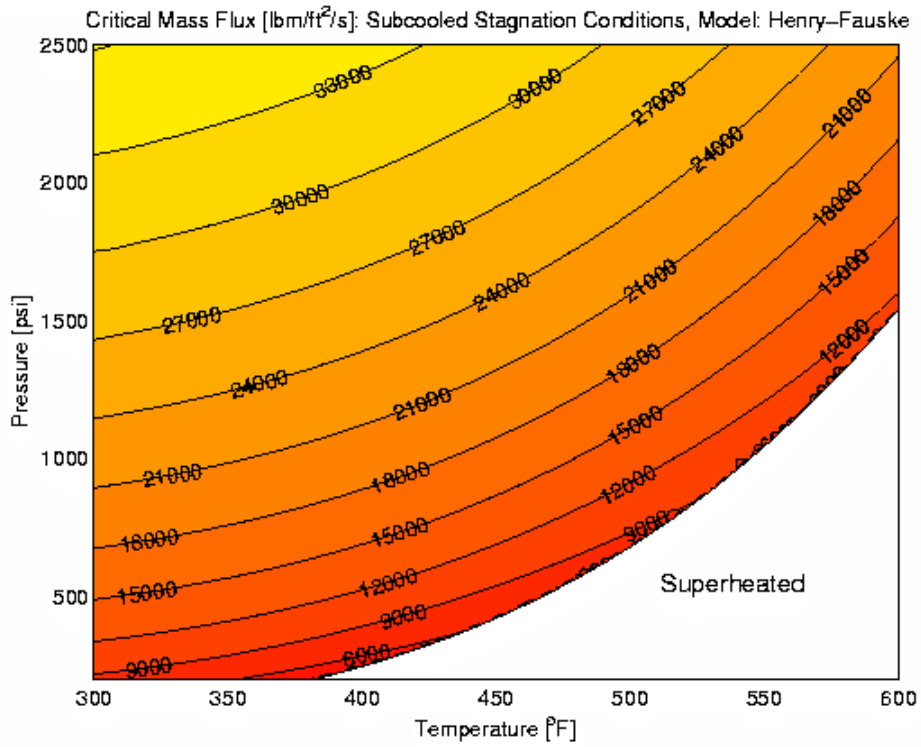


Figure I-6. Henry-Fauske Critical Mass Flux, Subcooled Stagnation

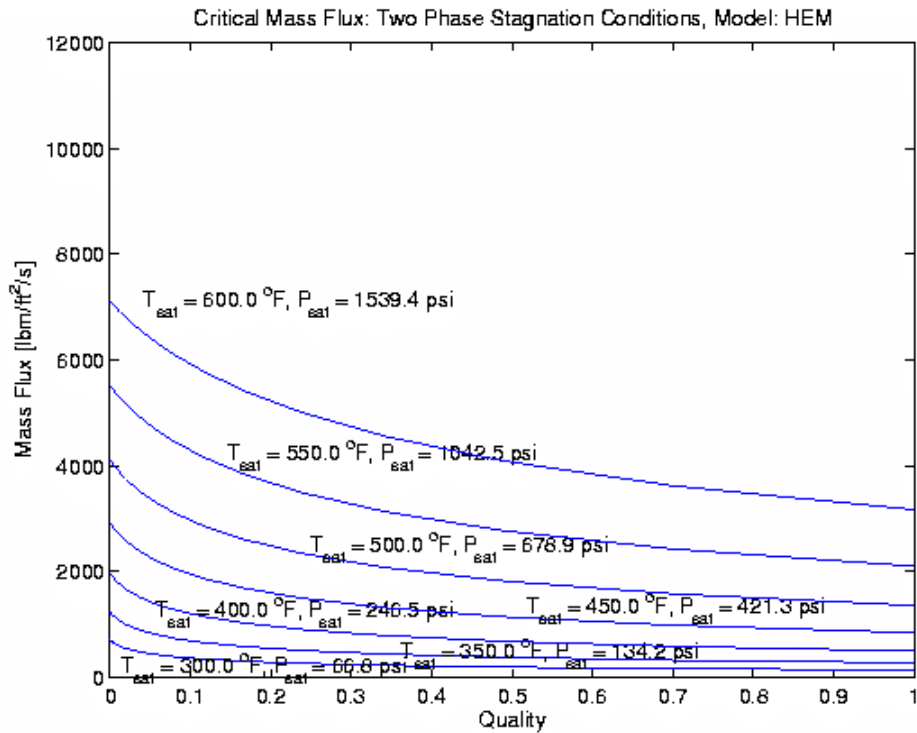
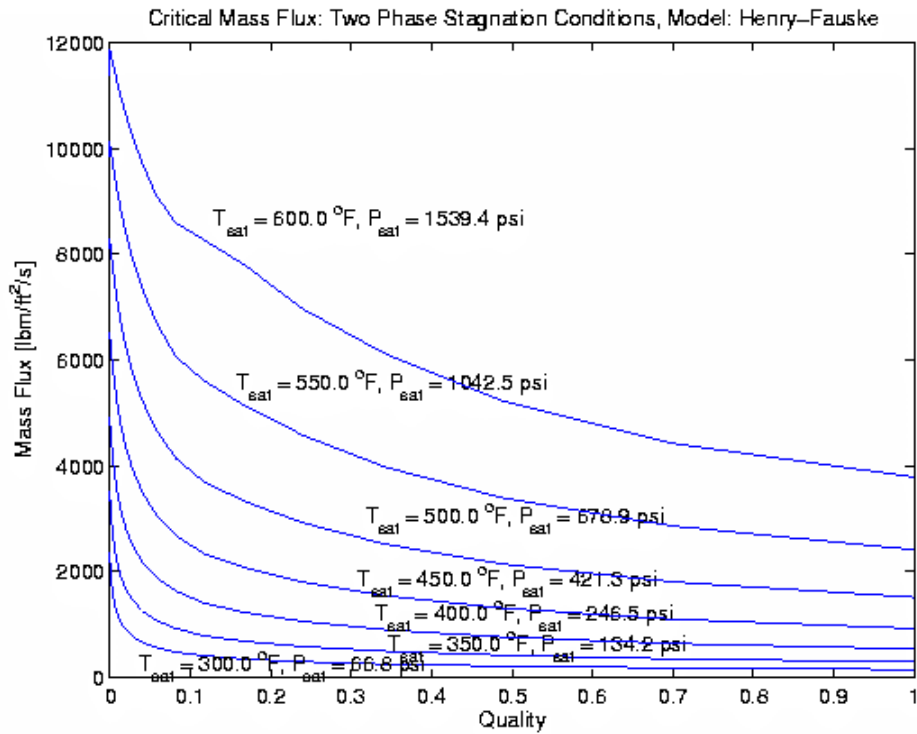
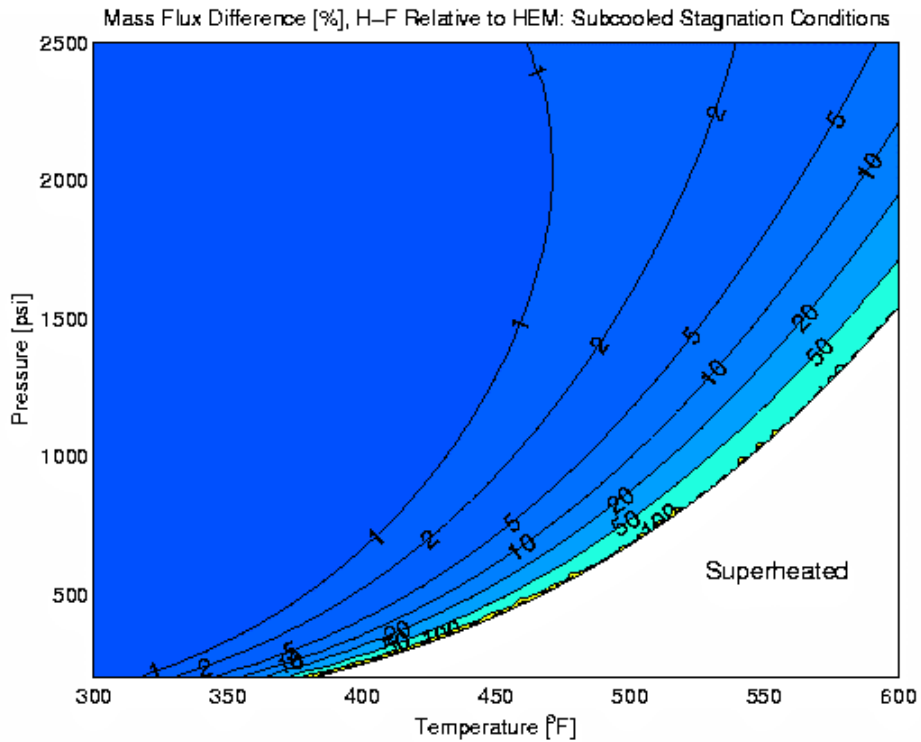


Figure I-7. HEM Critical Mass Flux, Saturated Stagnation



**Figure I-8. Henry-Fauske Critical Mass Flux, Saturated Stagnation**



**Figure I-9. Mass Flux Difference, Subcooled Stagnation**

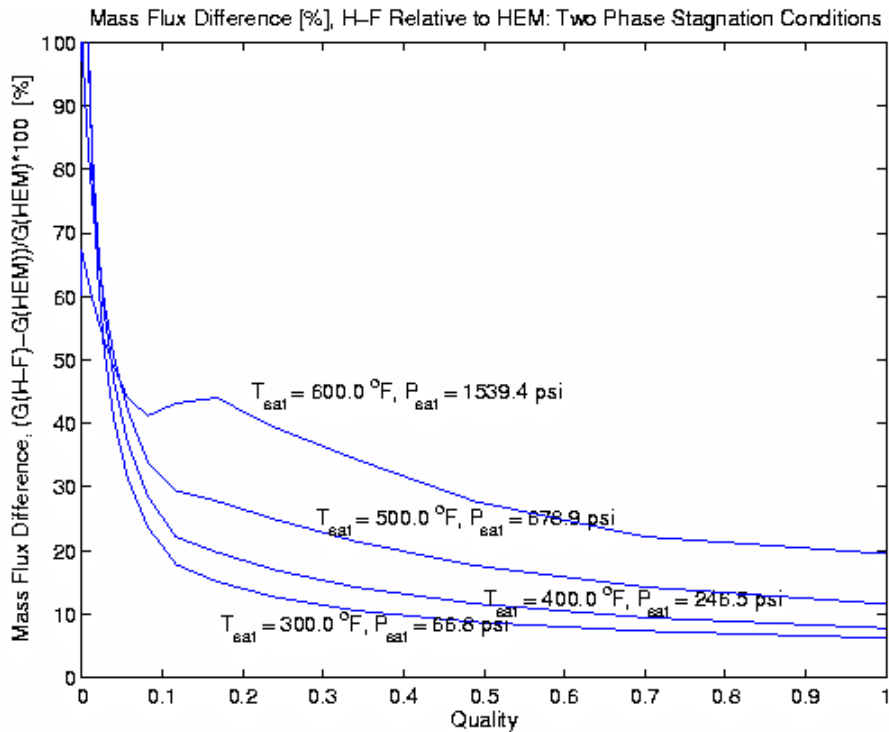


**Figure I-10. Mass Flux Difference, Saturated Stagnation**

If the advice of the standard is followed, then a significant discontinuity would be observed when the critical flow model transitions from the HEM to Henry-Fauske. The nature and magnitude of this discontinuity is explored further below. Although users of the jet model are in practice unlikely to observe this discontinuity, because during a blowdown, the transition might only occur after significant pressure drops, we see no compelling reason to preserve it. The issue then becomes one of selecting the model that offers the best fidelity to available data. The figures show that the HEM and Henry-Fauske offer comparable predictions for highly subcooled as well as high-quality two-phase conditions. This is to be expected because under these conditions, both models predict essentially monophasic fluid properties at the throat and the detailed treatment of the interphase heat- and mass-transfer rates offered by Henry-Fauske does not come into play. The benchmarking results reported in Ref. [Hen71] lead us to conclude that the Henry-Fauske model exhibits superior agreement to the data under low-quality two-phase and saturated liquid conditions. This alone is sufficient reason to adopt Henry-Fauske; further evidence may be found from an examination of a second major input to the ANSI jet model, the thrust coefficient.

### **1.5.2 Direct Evaluation of Thrust Coefficients**

The thrust coefficient  $C_T$  acts as a surrogate for the jet thrust force, which is not explicitly called for as an input to the ANSI model. This discussion will address only the steady-state thrust coefficient for frictionless, unrestricted flow, but its conclusions can be generalized to include those cases as well. Regardless of upstream conditions, the

thrust coefficient is used to correlate the thrust force  $T$ , upstream stagnation absolute pressure  $P_0$ , ambient pressure  $P_{amb}$ , and break area  $A_e$  by the expression

$$T = C_T(P_0 - P_{amb})A_e. \quad \dots\dots\dots(I-44)$$

Calculation of the thrust coefficient requires knowledge of local flow conditions at the break. Because these are unknown unless a critical flow model such as the HEM or Henry-Fauske is used to compute them, pp. 35 – 45 of the standard provide a series of correlations and figures that may be used as surrogates. Because both Henry-Fauske and the HEM were implemented for the current review, the results obtained from these models will be compared with the recommendations provided in the standard.

The thrust force may be computed by calculating the force that must be exerted to hold in static equilibrium a plate positioned normal to the flow directly at the break point. This thrust is given by

$$T = (P_e - P_{amb})A_e + \frac{1}{g_c} \rho_e v_e^2 A_e, \quad \dots\dots\dots(I-45)$$

where the static pressure  $P_e$ , fluid density  $\rho_e$ , and flow velocity  $v_e$  are evaluated at the exit. Combining the above equations yields an expression for the thrust coefficient:

$$C_T = \frac{1}{P_0 - P_{amb}} \left( \frac{1}{g_c} \rho_e v_e^2 + (P_e - P_{amb}) \right). \quad \dots\dots\dots(I-46)$$

Figure I-4 through Figure I-7 show thrust coefficients computed using pressures and fluid properties evaluated from the HEM and Henry-Fauske models. Regardless of the model, the value of  $C_T$  approaches 2.0 for incompressible, highly subcooled liquid and ~1.26 for saturated steam. These results agree with theory and are recommended for use in the standard.

For subcooled flashing upstream conditions, the standard on p. 42 recommends use of the curve fits presented by Webb [WEB76]. Based on an enthalpy normalization factor

$$h^* = \frac{h_0 - 180}{h_{sat} - 180}, \quad \dots\dots\dots(I-47)$$

where  $h_0$  [Btu/lbm] is the upstream stagnation enthalpy and  $h_{sat}$  [Btu/lbm] is the saturated water enthalpy at the stagnation pressure, the correlation is evaluated as

$$C_T = 2.0 - 0.861h^{*2} \text{ for } 0 \leq h^* < 0.75 \quad \dots\dots\dots(I-48)$$

and

$$C_T = 3.22 - 3.0h^* + 0.97h^{*2} \text{ for } 0.75 \leq h^* \leq 1.0. \quad \dots\dots\dots(I-49)$$

For saturated or superheated steam, the standard recommends a thrust coefficient of

$$C_T = 1.26 - P_{amb}/P_0 . \quad \dots\dots\dots(I-50)$$

For two-phase steam-water mixtures, the standard provides only a figure that does not address relevant PWR break conditions, and for nonflashing water jets with temperatures less than the saturation temperature at ambient pressure and pressures greater than ambient, the standard recommends that

$$C_T = \frac{2}{1 + fL/D} , \quad \dots\dots\dots(I-51)$$

where the Fanning friction factor  $f$  is normally assumed to be zero for conservatism. The ratio  $L/D$  represents a dimensionless flow-path length based on the characteristic length and diameter of the piping between the assumed thermodynamic reservoir and the break location.

Webb claims, and our calculations verify, that his correlations agree with values computed from the Henry-Fauske model to within 3% for upstream stagnation pressures ranging from 300 to 2400 psia. The standard does not clearly state this range of applicability. Webb's correlation is recommended when a computational implementation of a critical flow model is unavailable, but two inconsistencies require clarification.

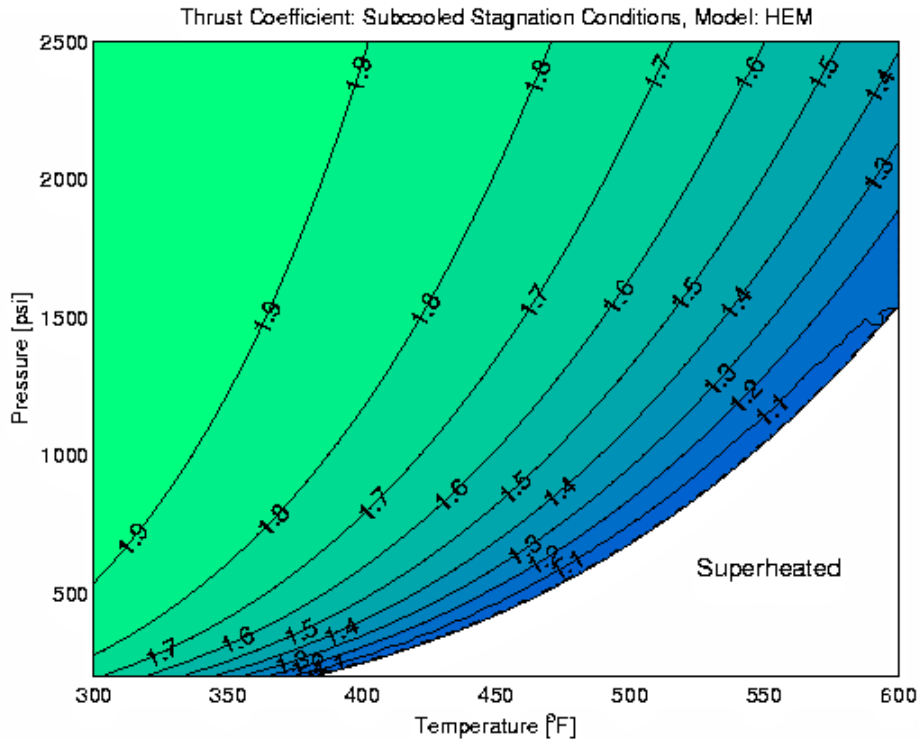


**Figure I-11. HEM Thrust Coefficient, Subcooled Stagnation**

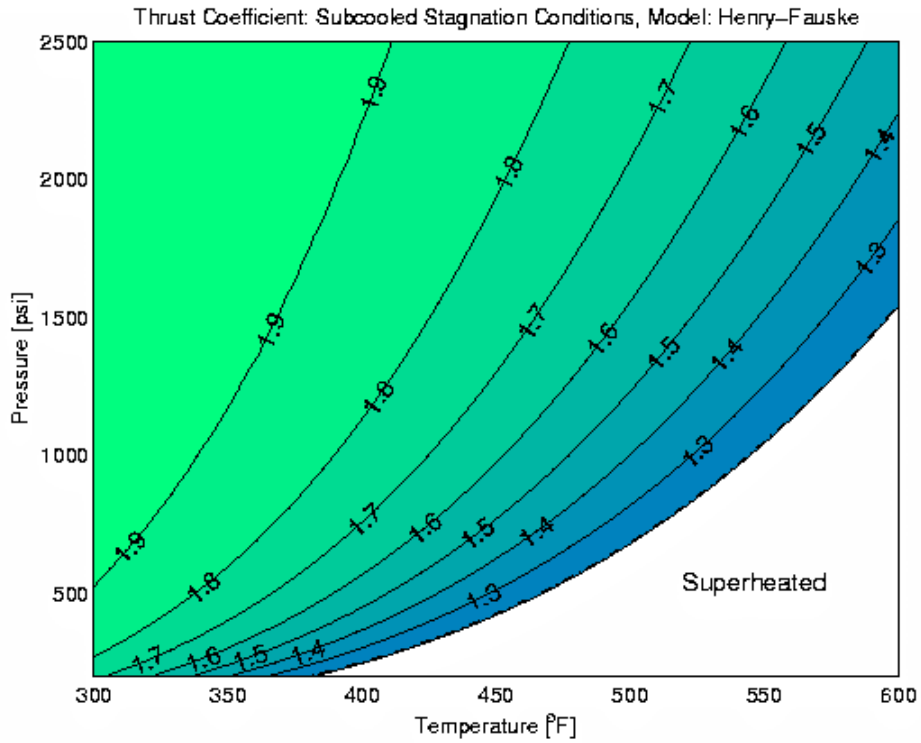


Figure I-12. Henry-Fauske Thrust Coefficient, Subcooled Stagnation

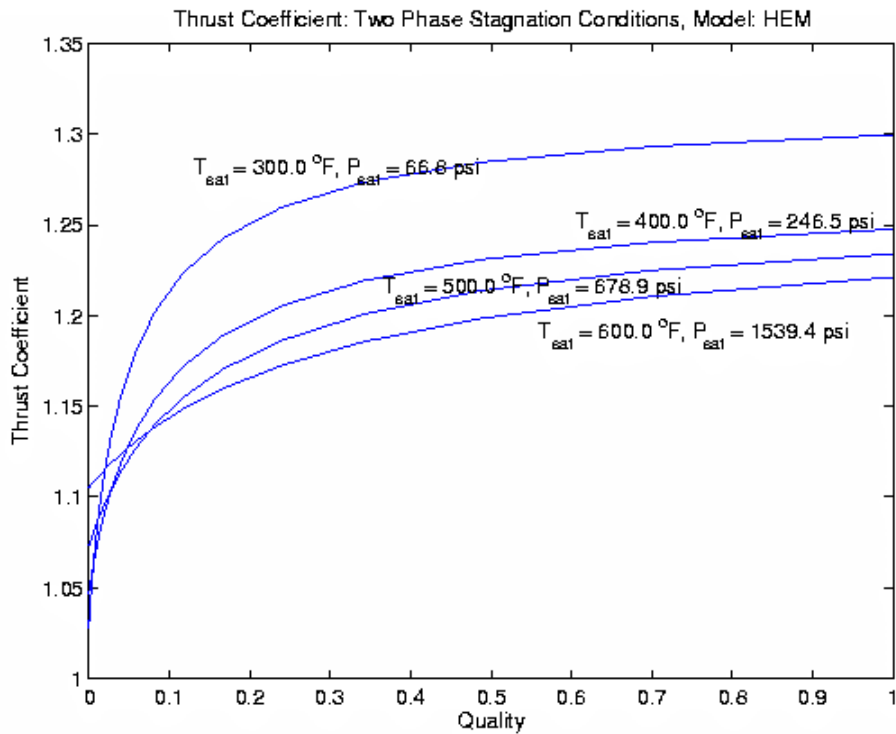
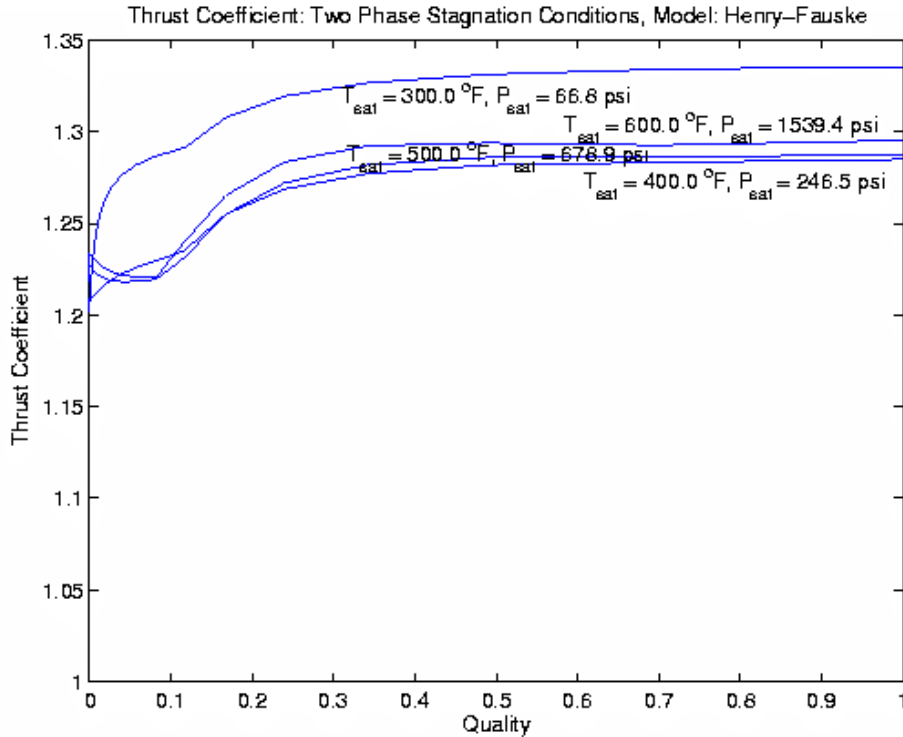


Figure I-13. HEM Thrust Coefficient, Saturated Stagnation



**Figure I-14. Henry-Fauske Thrust Coefficient, Saturated Stagnation**

In presenting Webb’s model, the standard neglects to clarify the “180” figure against which the enthalpy is nondimensionalized. This is, in fact, the enthalpy of saturated water at atmospheric pressure, 14.7 psi. It may be justifiably claimed that, during a blowdown, the ambient containment pressure might vary from below atmospheric to significantly above atmospheric. Changes in  $P_{amb}$  cannot be accounted for by Webb’s model; however,  $C_T$  evaluated from the force balance varies weakly with  $P_{amb}$ . This effect is not large: even for highly subcooled conditions at the lower end of the range of validity of Webb’s correlation,  $P_0 = 300 \text{ psia}$ , neglecting  $P_{amb}$  altogether changes the thrust coefficient evaluated from the force balance by less than 5%.

The standard also places insufficient emphasis on the fact that Webb’s correlation is obtained from calculations using the Henry-Fauske model. Because this is the case, employing HEM-derived mass fluxes with thrust coefficients obtained from this correlation propagates of a significant inconsistency. Figure I-8 shows that significant deviation exists between thrust coefficients computed from the outlet conditions provided by the two critical flow models. The use of Henry-Fauske-derived thrust coefficients with HEM mass fluxes will result in overprediction of damage radii. This follows because the larger Henry-Fauske thrust coefficient implicitly imposes a higher flow density, velocity, and/or static pressure at the break plane.

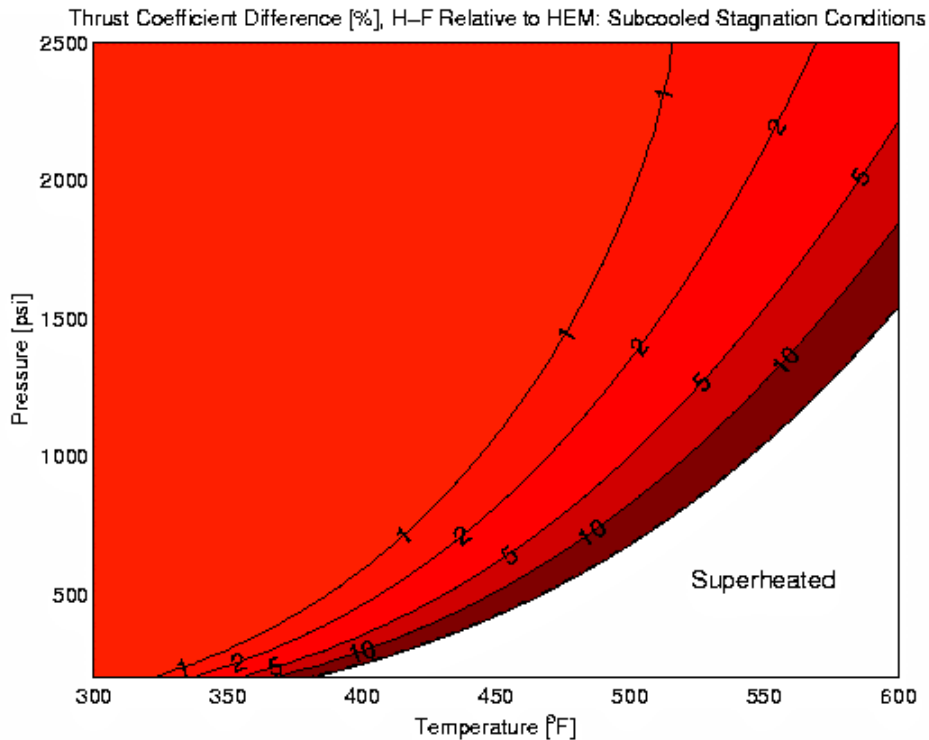


**Figure I-15. Thrust Coefficient Difference, Subcooled Stagnation**

### I.5.3 Effects of Flow Models on Jet Behavior

While the sensitivity of the jet pressure contour map in its entirety to variations in  $C_T$  is too complicated to permit analytic treatment, the effect of variation of  $C_T$  on conditions at the asymptotic plane can be used for illustration. Equation (I-43) shows that the jet area  $A_a$  at the asymptotic plane is inversely proportional to  $C_T$ . However, from conservation of mass, Equation (I-40), the average flow velocity at the asymptotic plane  $v_a$  is inversely proportional to  $A_a$  and, thus, directly proportional to  $C_T$ . This conclusion can be drawn because the average fluid density  $\rho_a$  at the asymptotic plane depends, in the ANSI formulation, only upon upstream stagnation conditions. The dynamic pressure of the fluid, which is proportional to the square of its velocity, thus varies as  $C_T^2$ . The results of decreased jet cross sectional area and increased velocity from the larger Henry-Fauske thrust coefficient will be a narrower, more penetrating jet and larger volume-equivalent radii at a given damage pressure.

In fact, it can be seen from Figure I-6 that the thrust coefficient for upstream conditions at or near saturation as derived from the HEM is significantly lower than the value of 1.26 recommended in Figure B-5 of the Standard. The inconsistency inherent in use of the 1.26 value with the HEM mass flux would again result in overprediction of volume-equivalent radii. This additional consideration strengthens our recommendation that the Henry-Fauske method be employed for all flow regimes when performing the calculations outlined in the standard.

As mentioned above, the critical mass flux  $G_e$  derived from the HEM will be smaller, significantly so for stagnation conditions lying near the liquid saturation line in  $(P, h)$  space, than that obtained from Henry-Fauske. Because this is the case, it is also useful to address the behavior at the asymptotic plane when  $G_e$  is varied with  $C_T$  being held constant. Following the same reasoning pursued above when the thrust coefficient was varied, we see that the jet area at the asymptotic plane varies as  $G_e^2$ . The average jet velocity at that location  $v_a$ , on the other hand, behaves as  $v_a = kG_e/A_a$  so that  $v_a \sim 1/G_e$ . Thus, a seemingly paradoxical conclusion is reached, namely that reducing the mass flux while holding the thrust coefficient constant increases the velocity at the asymptotic plane and might *increase* the volume-equivalent radii.

Although this thought experiment is not conclusive or comprehensive – the location of the asymptotic plane, for instance, also depends on  $G_e$  and  $C_T$  and has not been taken into account – numerical computations verify its conclusions. Table I-1 shows critical flow model results for five of the upstream conditions given in Table I-2. The conditions selected from that table are #8, PWR Hot Leg Initial; #1, PWR Cold Leg Initial; #2, PWR Cold-Leg Blowdown; #9, BWR Hot-Leg; and #11, Main Steam Line. All three PWR stagnation states are subcooled; the BWR state is two-phase with a quality of 0.15 and the steam line case is superheated by 35°F. In addition to the mass flux  $G_e$ , thrust coefficient  $C_T$  and discharge velocity  $v_e$  obtained, the volume-equivalent damage radii for the 10 and 150 psig contours are also shown. It might be intuitively expected that the Henry-Fauske model is the more conservative when calculating damage radii because it predicts critical mass fluxes and thrust coefficients that are greater than those of the HEM, but, as shown in the table, particularly for initial conditions nearing saturation, this is not the case.

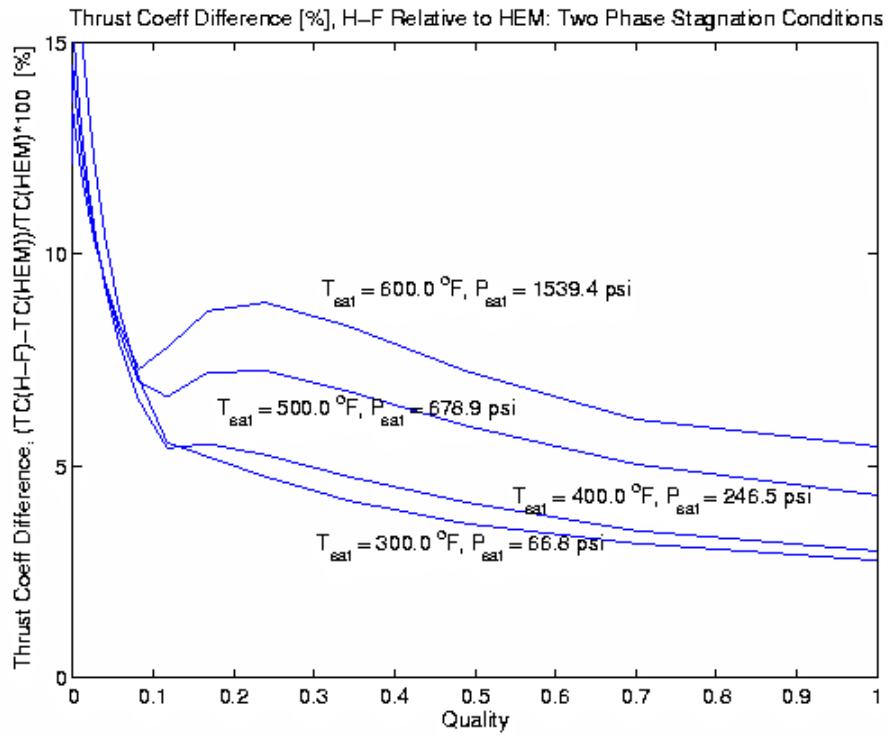


**Figure I-16. Thrust Coefficient Difference, Saturated Stagnation**

**Table I-1. Critical Flow Model Results and Their Effect on Volume-Equivalent Damage Radii**

	Critical Mass Flux $G_e$ [lbm/ft <sup>2</sup> /s]		Thrust Coefficient $C_T$ [--]		Break Flow Velocity $v_e$ [ft/s]		150-psig* Damage- Pressure Radius [pipe diameters]		10-psig* Damage- Pressure Radius [pipe diameters]	
	HEM	H-F	HEM	H-F	HEM	H-F	HEM	H-F	HEM	H-F
1. Cold Leg Initial (2250 psia, 530 F)	24850	25330	1.62	1.64	1.63	527	1.48	1.48	12.00	12.04
2. Cold-Leg Blowdown (393 psia, 291 F)	13370	13390	1.88	1.89	1.90	232	0.96	0.96	4.42	4.43
8. Hot Leg Initial (2250 psia, 630 F)	11840	15400	1.17	1.28	1.28	296	1.60	1.59	11.14	11.07
9. BWR Hot Leg (1040 psia, 550 F, X = 0.15)	3920	5260	1.16	1.26	N/A	178	1.11	1.12	7.81	7.80
11. Main Steam Line (910 psia, 570 F)	1800	N/A	1.24	N/A	N/A	464	1.08	N/A	7.58	N/A

\* Damage-pressure radii are given as multiples of the break diameter. They are obtained by constructing spheres with volume equal to the volume enclosed by a given jet stagnation pressure contour. See Section I.3 for further elaboration.

\*\* Shown for purposes of comparison only; not used in damage-pressure-radius calculations given in this table.

## I.6 SAMPLE CALCULATIONS

The ANSI model presented in the previous sections for predicting stagnation pressures in an expanding jet was implemented in a MATLAB routine called ANSIJet (see Attachment 1 to this appendix). This programming language was selected for convenient interface with steam-table routines available from NIST. Several cases relevant to both PWR initial break and blowdown conditions were evaluated. Two generic BWR state points were also evaluated, as were three cases applicable to steam line flow in secondary loops. Two of these relate to a single-pass Babcock & Wilcox steam generator discharging superheated (by ca. 35° F) steam; the third applies to a Combustion Engineering U-tube heat exchanger and is assumed to yield saturated steam. These conditions are defined in Table I-2 for later reference by case number. Note that Figure I-1 corresponds to the cold-leg initial break condition defined as Case #1.

**Table I-2. Comparative Calculation Set Using ANSI Jet Model**

Case #	Description	System Stagnation Conditions		
		$P_o$ (psia)	$T_o$ (°F)	Quality
1	cold leg initial <sup>1</sup>	2250	530	Subcooled
2	cold-leg blowdown <sup>1</sup>	393	291	Subcooled
3	cold-leg blowdown <sup>1</sup>	857	351	Subcooled
4	cold-leg blowdown <sup>1</sup>	1321	411	Subcooled
5	cold-leg blowdown <sup>1</sup>	1786	471	Subcooled
6	10% greater pressure than Case 1	2475	530	Subcooled
7	cold leg initial <sup>2</sup>	2250	540	Subcooled
8	hot leg initial <sup>3</sup>	2250	630	Subcooled
9	BWR hot leg <sup>4</sup>	1040	550	0.15
10	BWR cold leg <sup>4</sup>	1040	420	Subcooled
11	main steam line (MSL): Babcock & Wilcox (B&W) <sup>4</sup> – full power	910	570	Superheated
12	B&W MSL: design conditions <sup>4</sup>	1075	603	Superheated
13	MSL: Combustion Engr. Calvert Cliffs <sup>5</sup>	846	525	1.0

<sup>1</sup> From reference [RAO0]

<sup>2</sup> From reference [NEI04]

<sup>3</sup> From reference [DUD76]

<sup>4</sup> From reference [RAH92]

<sup>5</sup> From reference [LOB90]

Jet-pressure isobars for Cases 1 through 6 were integrated over a wide range of values and converted to equivalent spherical diameters. These results are presented in Fig. I-17. Recall that the ANSI-model stagnation pressure is being used as a correlation parameter that corresponds to observed damage in debris generation tests. Use of this

correlation is the reason that the Figure I-17 abscissa is labeled as “Damage Pressure.” Case 1 represents a previously studied hydraulic condition [RAO02] that will be used as the reference case. Reading from the figure, a damage pressure of 10 psig corresponds to an equivalent jet radius of approximately 12 pipe diameters. Note that equivalent radii climb sharply for damage pressures below 20 psig.

This set of calculations suggests that the state-point pressure of the jet dominates the determination of isobar volumes. Other cases that are not shown in Figure I-17 were bounded by Case 1. Case 7, the nominal PWR cold-leg condition recommended in the GR, was almost indistinguishable from Case 1. Case 8, a nominal hot-leg break condition, was also bounded by the reference case except at damage pressures greater than 120 psig. Hot-leg conditions are much closer to saturation (630°F vs. 653°F); therefore, the shapes of the pressure contours change near the core. Case 6 was run as a perturbation check for plants that may at times have higher operating pressures than the nominal value of 2250 psig. Although the pressure increase was 10% higher than the reference, the maximum deviation in spherical volume was only 8%; therefore, a linear adjustment for higher pressure would be conservative in the absence of a full jet-model analysis.

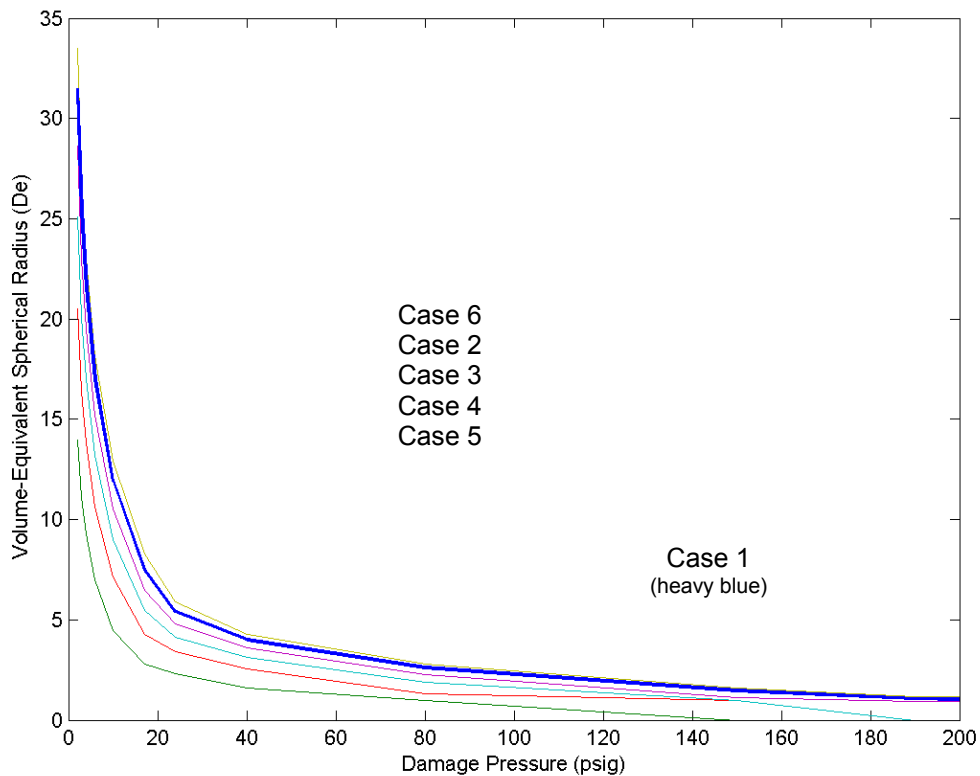


**Figure I-17. Comparison of ANSI Jet-Model Equivalent Spherical Radii for Six Initial Break Conditions**

The damage radii associated with the BWR hot-leg and cold-leg conditions of Cases 9 and 10 are shown in Figure I-18. Given the lower stagnation pressures pertinent to BWR coolant, the equivalent radii are, as expected, smaller than was the case for PWR

conditions at comparable values of damage pressure. The radii obtained for the three steam line cases are given in Figure I-19. Two of these, Cases 11 and 13, are specified as representative of full power operating conditions. The third, Case 12, is a design specification included to serve as a conservative bounding scenario. Given that the thrust coefficient is nearly invariant at a value near 1.26 for high-quality two-phase and superheated upstream conditions, it appears reasonable to expect damage radii in such regimes to respond linearly to variation in the stagnation pressure. A pressure contour plot for the steam line break condition is provided in Figure I-20. This figure compares to Figure I-1 for PWR cold-leg stagnation conditions. One of the subtle differences between these figures is the higher centerline pressure exhibited by the MSL case to axial distances of about 30 pipe diameters. The steam flow exhibits a narrower jet that is higher-velocity at the centerline, leading to a greater dynamic contribution to the stagnation pressure. Differences in the initial pressure should also be considered when visually comparing Figures I-1 and I-20.

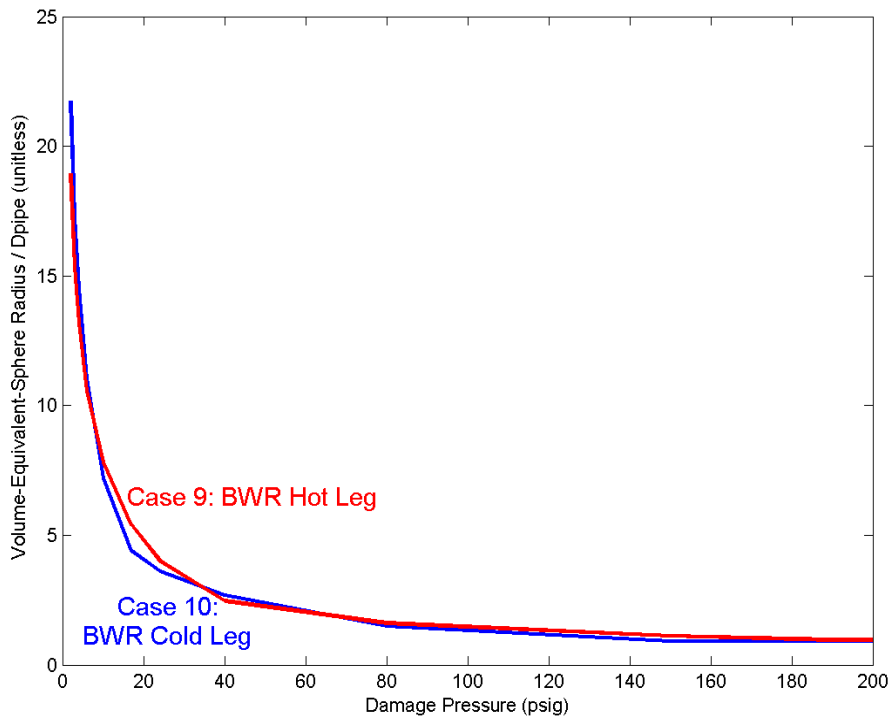


**Figure I-18. Comparison of ANSI Jet-Model Equivalent Spherical Radii for BWR Break Conditions**

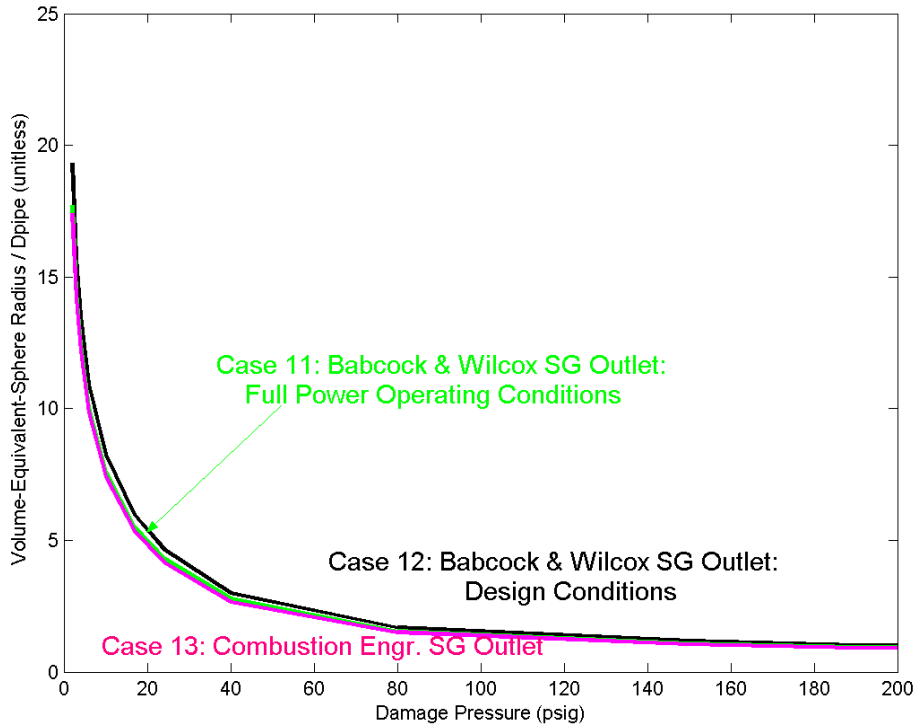


**Figure I-19. Comparison of ANSI Jet-Model Equivalent Spherical Radii for Main Steam Line Break Conditions**

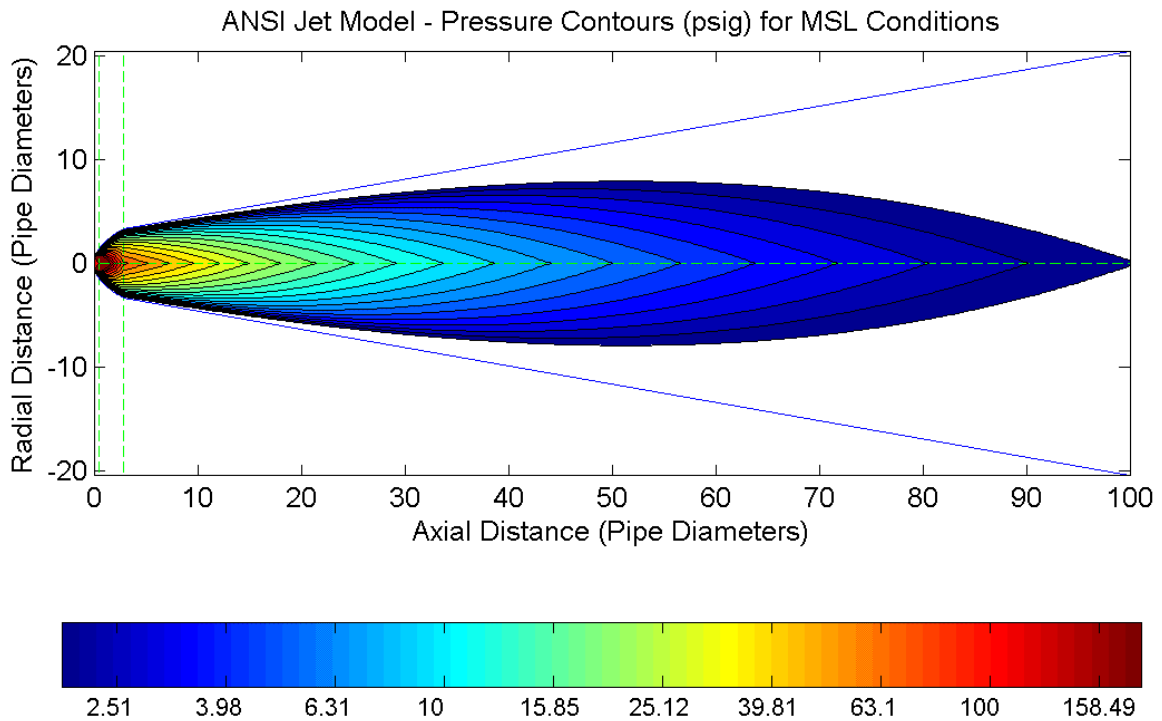


**Figure I-20. ANSI Jet-Model Stagnation Pressures for MSL Break Conditions (570°F, 910 psia)**

Other useful information can be extracted from the jet model in addition to equivalent spherical diameters derived from spatial volume integrals. Appendix D of the ANSI standard suggests that target temperatures can be estimated by evaluating a thermodynamic state point using the jet pressures  $P_j$  and the initial enthalpy  $h_0$ . Presuming that the model supplies realistic, nonisentropic impingement pressures (at least in the longitudinal direction), this approach will give the temperature of the stationary fluid striking the surface of a large target. Actual target temperatures might vary with internal heat conduction properties and external drag coefficients that affect aerodynamic heating, but it is instructive to compute this approximation nonetheless. Figure I-21 illustrates the isotherm plot corresponding to Case 1 for the reference cold-leg break.

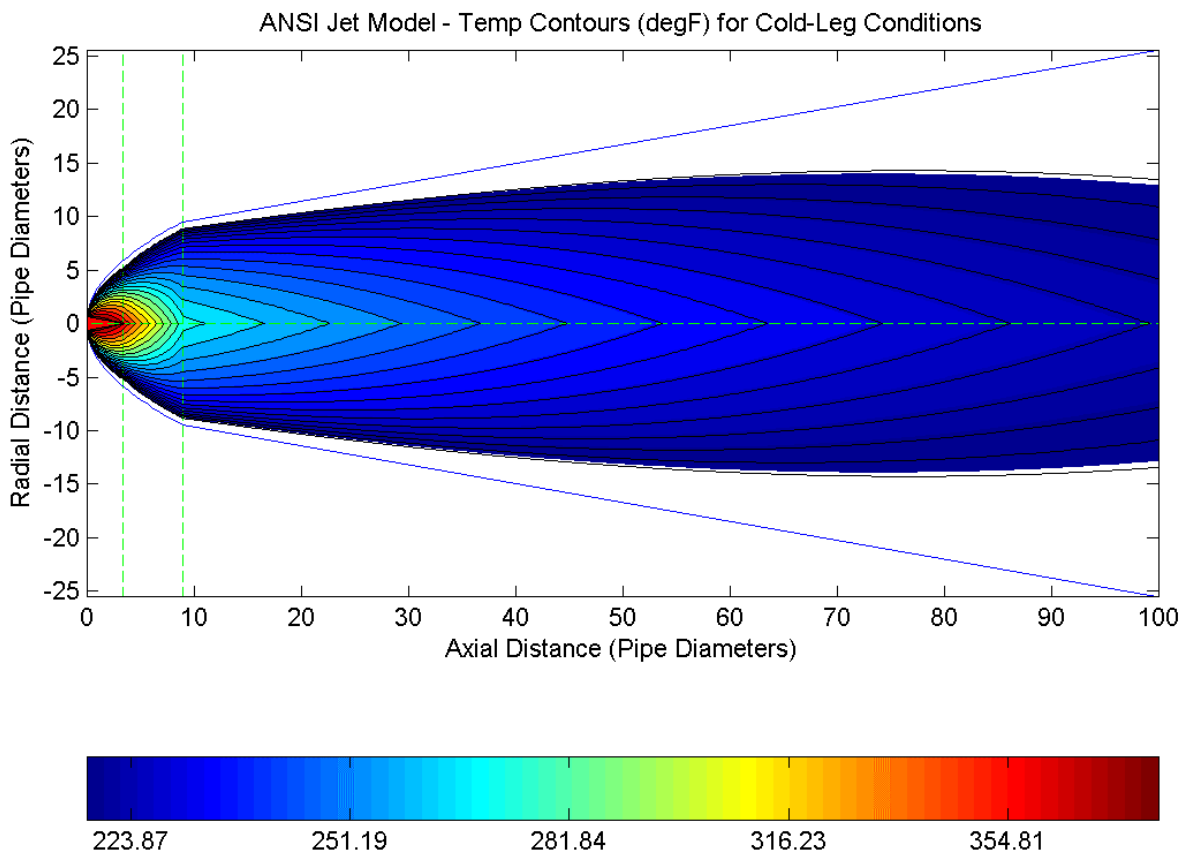


**Figure I-21. Isotherm Contours for the Reference Cold-Leg Break at 2250 psia and 530°F**

The somewhat surprising attribute of the isotherm map is how slowly the impingement temperature changes beyond the range of 10 to 15 pipe diameters downstream of the break. For potential debris-generation mechanisms that are suspected to have important thermal responses, this information can directly benefit both the specification of relevant test parameters and the interpretation of existing test data. For example, a test performed at 280°F that exhibits good damage resistance demonstrates substantially

less spatial vulnerability to high-temperature jets than a test performed at 220°F. As with pressure contours, isotherm volumes can also be mapped to equivalent spherical volumes, and because the ANSI model exhibits spatial monotonicity (uniformly increasing or decreasing in every direction) in all physical jet properties, there is a unique correspondence between pressure, temperature, and contour volume.

Another impingement-state parameter of interest is the fluid quality. There has been a long-standing debate regarding the potential for enhanced debris generation in the presence of entrained water droplets compared with that observed for high-quality steam and for air-jet surrogates. While the ANSI model cannot answer this concern, it may offer information on the spatial extent of the phenomena. Subject to the same interpretations and approximations as those discussed for impingement temperature, the jet quality can also be evaluated at  $P_0$  and  $h_0$ . Contours of equal two-phase steam quality are illustrated in Figure I-22 for the reference cold-leg break. Similar to temperature, the fluid quality changes slowly beyond a range of 10 to 15 pipe diameters and maintains a nominal value between 0.25 and 0.35. This range would be considered low-quality steam for turbine generator applications and might be viewed with concern for its potential erosion effects on stainless steel rotor blades. Certainly, the time regimes of jet impact and in-service steam components are drastically different, but the potential damage mechanisms are the same.

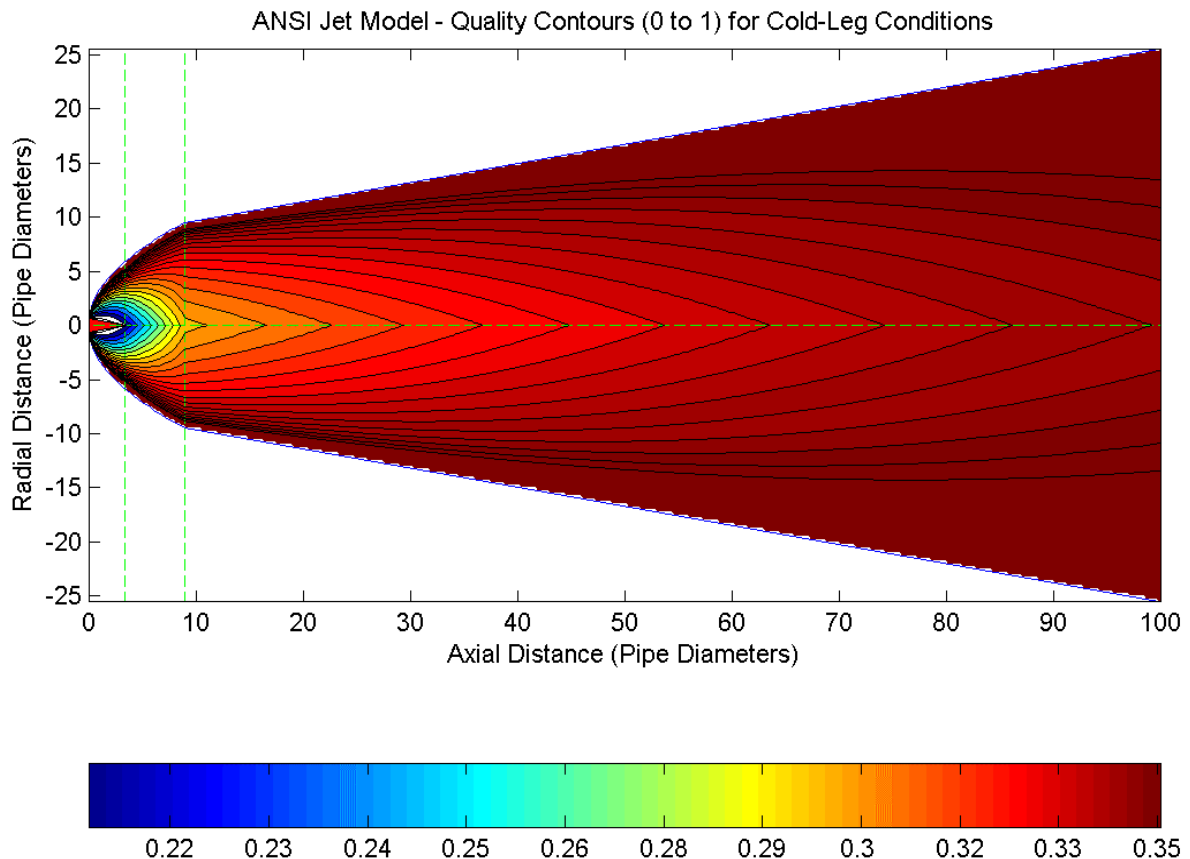


**Figure I-22. Contours of Equivalent Steam Quality for the Reference Cold-Leg Break at 2250 psia and 530°F**

The thermodynamic treatment of two-phase saturated conditions in the ANSI standard is inherently a homogeneous mass-mixture model. That is, the two-phase mixture is considered to be a single fluid with equivalent mass-weighted thermodynamic properties. This assumption, along with that of equal phase velocities in the jet, is justified by Lahey and Moody [LAH84]. Therefore, void fractions could be estimated from the local pressures and qualities. Under this assumption, it was found that the qualities shown in Figure I-19 would correspond to void fractions greater than 0.95 for all regions of the jet apart from the core. While Figure I-19 could be separated into the fluid and vapor mass fractions using the saturation properties and the definition of quality, the real issue of momentum transfer to a target could not be addressed with convincing accuracy. Theoretical treatments of two-phase transport introduce concepts of condensate nucleation, interphase velocities, droplet drag coefficients, and void fraction (space between droplets) that are difficult to measure experimentally. Pursuing this analysis with the present ANSI model would exceed the scope of its purpose and fidelity.

In summary, Table I-3 presents a set of concomitant values for pressure, temperature, quality and equivalent spherical radius that characterize the approximate impingement conditions in an expanding jet generated by a cold-leg break at 2250 psia and 530°F. With respect to equivalent spherical diameter, this reference case is observed to bound all break conditions of interest for a PWR accident analysis. Table I-4 lists intermediate parameter values computed by ANSJet for the reference break conditions. This information may be useful for comparisons of independent implementations of the jet model.

**Table I-3. Summary of Jet Properties for the Reference Cold-Leg Break**

$P_{jet}$ (psig)	$T_{jet}$ (°F)	$Q_{jet}$	$R_{sphere}$
2	218.7	0.35	31.5
3	221.8	0.34	25.4
4	224.6	0.34	21.6
6	230.0	0.34	17.0
10	239.6	0.33	11.9
17	253.7	0.32	7.5
24	265.5	0.31	5.4
40	287.0	0.29	4.0
80	324.2	0.26	2.6
150	366.1	0.21	1.5
190	384.0	0.20	1.1
2250	530.0	0.00	0.9

**Table I-4. Intermediate Parameters Computed by the ANSI Jet Routine for the Reference Cold-Leg Break Conditions**

Vessel Pressure	P0	[psia]	2250
Vessel Temp	T0	[deg F]	530
Vessel Quality	X0	[-]	-0.430084
Vessel Density	r0	[lbm/ft <sup>3</sup> ]	48.0879
Vessel Enthalpy	h0	[Btu/lbm]	522.455
Sat Temp at P0	Tsat	[deg F]	653.014
Liq Sat Enth at P0	hf	[Btu/lbm]	700.946
Vap Sat Enth at P0	hg	[Btu/lbm]	1115.96
Ambient Pressure	Pamb	[psia]	14.7
Pres at Asym Plane	Pa	[psia]	14.7
Dens at Pa, h0	rma	[lbm/ft <sup>3</sup> ]	0.105653
Computed Thrust Coeff	TC	[-]	1.64413
Crit Mass Flux	Ge	[lbm/ft <sup>2</sup> /s]	25329.2
Tsat at Pamb	Tsatamb	[deg F]	212.238
Liq Sat Enth at Pamb	hfamb	[Btu/lbm]	180.176
Vap Sat Enth at Pamb	hgamb	[Btu/lbm]	1150.28
Degrees Subcooling	delTsub	[deg F]	123.014

## I.7 SUMMARY CRITIQUE OF THE ANSI JET MODEL

Appendix I provides an exposition of the ANSI model and addresses several points where the model may be insufficiently clear or may suffer from an inconsistency. The major issues raised in the Appendix are summarized below; where applicable, recommendations for remediation are provided.

- The pressure distribution produced by the model exhibits a discontinuity across the boundary of the core. Within the core, the stagnation pressure is assumed to equal the upstream pressure  $P_0$ ; the discontinuity has been observed to reach an order of magnitude for certain upstream conditions.
- Although not explicitly stated in the model, the jet pressure distribution, which falls to zero in the far field, must be interpreted as representative of local impingement gauge pressures.
- The jet pressure at the centerline, however, remains nonzero for any finite value of the axial penetration distance. This exaggerates pressure isobar volumes and causes volume-equivalent spherical damage radii to approach infinity as the damage pressure goes to zero.
- The pressure distribution has evidently been formulated such that the thrust force is correctly recovered only for targets oriented normal to the flow direction at the orifice. Therefore, the model may not be a good approximation to free-field expansion: it may not accurately predict local conditions at points away from the jet centerline, where the flow velocity on such a normally-oriented plate would exhibit a significant tangential component. This concern is not

addressed by the application of a shape factor as outlined in Appendix D of the ANSI report.

- The above point has further ramifications for the applicability of the model to small targets. Since the stagnation pressure field produced by the model was developed to reproduce loadings on large flat targets, it is inaccurate to apply the stagnation pressures to small and/or non-flat objects. One could bound the true conditions by computing local static pressures as well; however, knowledge of the local velocity field and of the characteristics of the two-phase jet flow that are beyond the scope of the ANSI model would be required.
- A discontinuity in the slope of the isobars exists between Zones 2 and 3. This discontinuity is clearly evident in Figure I-1. The sharp terminal points of pressure isobars at the axial centerline also suggest that more attention could be given to the behavior of first spatial derivatives.
- The assumption of isentropic and/or isenthalpic expansion should be made with caution. For instance, stagnation conditions at the asymptotic plane are evaluated assuming isenthalpic behavior, implying no energy loss to the environment. In general, however, the isentropic assumption appears to be applied to the expanding jet. For a discussion of the limitations of these assumptions see Ref. [WIT02].
- Although it was analytically confirmed that all characteristic lengths in the problem scale linearly with the break diameter  $D_e$ , it is recommended that users implement the formulation of the model presented herein, as it has been nondimensionalized with respect to this quantity.
- The notation adopted by the standard for the thrust coefficient is evidently inconsistent:  $C_T$ ,  $C_{Te}$ , and  $C_{Te}^*$  all appear in the equations describing the pressure distribution for the various jet zones. These forms must all refer to a single numeric value if the pressure equations are to be piecewise continuous between zones.
- The ANSI model presents an expression for the jet area at the asymptotic plane that rests upon the assumption that the average flow static pressure at that location equals the ambient pressure  $P_{amb}$ . Elsewhere in the ANSI model, however, the asymptotic plane static pressure is assigned a value that may be less than  $P_{amb}$ .
- The standard advises users to implement a critical flow model, either the homogeneous equilibrium model (HEM) or the Henry-Fauske model, to obtain the jet mass flux  $G_e$ . Users not having such a model available may estimate  $G_e$  from Figure C-4 of the ANSI report; however this figure only covers stagnation conditions extending to 2000 psi and 50°F of subcooling, leaving certain states (e.g., cold leg conditions in many PWRs) unaddressed. Given the additional inaccuracies that may be introduced by reading from the figure, it

is strongly recommended that a critical flow model be implemented for use with the jet model.

- The standard recommends that Henry-Fauske critical flow model be used for subcooled vessel conditions and the HEM for saturated conditions. This would introduce a strong discontinuity as the liquid saturation point is crossed. Therefore, since Henry-Fauske is evidently in better agreement with the data for both subcooled and two-phase conditions, exclusive use of this model is recommended.
- An implied discontinuity exists across the break plane, as the ANSI model assumes that fluid in the core is in equilibrium at the upstream stagnation pressure and quality. This assumption contradicts aspects of both the HEM and Henry-Fauske models.
- The correlation recommended by the standard for use in calculating the thrust coefficient  $C_T$  for subcooled conditions applies only to Henry-Fauske derived mass fluxes. This is not made clear in the standard. Also left unclear is the assumption inherent in the correlation that ambient conditions are at standard pressure. Therefore, this correlation should not be used in conjunction with HEM mass fluxes, and users of the standard should bear in mind that the correlation is not strictly validated for ambient conditions deviating from those of the standard atmosphere. The error is small, though, for most upstream pressures of interest in the present analysis.
- No analytic correlation is provided by the standard for the thrust coefficient relevant to saturated steam-water mixtures. Within the standard, users may only consult Figure B-5 to visually gauge an approximate value. Another recourse would be to consult the thrust coefficient contour plots presented in this appendix, or better, implement a critical mass flux model to enable direct calculation of mass flux and thrust coefficient via the Henry-Fauske model.
- Users should be aware that one desired result of the model, volume-equivalent spherical damage-pressure radii, can behave nonintuitively as certain upstream conditions are varied. For instance, the PWR hot leg and cold leg results presented in Table I-1 of this appendix show that the flow from the hot leg break exhibits a lower mass flux and thrust coefficient than that from the cold leg. Nonetheless, the damage radii are roughly comparable, with radii for the hot leg break being greater than those of the cold leg for higher damage pressures and smaller for lower damage pressures. These results, which follow from variations in the flow velocity and density at the break, reinforce the importance of not eliminating lower-energy break points *a priori* when conducting ZOI analyses.

## I.8 REFERENCES

- [ANS88] “American National Standard: Design Basis for Protection of Light Water Nuclear Power Plants Against the Effects of Postulated Pipe Rupture,” American Nuclear Society, ANSI/ANS-58.2-1988, October 1988.
- [DUD76] Duderstadt, J. J., Hamilton, L. J., *Nuclear Reactor Analysis*, Wiley and Sons, New York, New York (1976).
- [RAO02] Rao, D. V., Ross, K. W., Ashbaugh, S. G., “GSI-191: Thermal-Hydraulic Response of PWR Reactor Coolant System and Containments to Selected Accident Sequences,” prepared for the U.S. Nuclear Regulatory Commission by Los Alamos National Laboratory, NUREG/CR-6770, LA-UR-01-5561 (August 2002).
- [NEI04] “Pressurized-Water-Reactor Sump Performance Evaluation Methodology,” prepared by the Nuclear Energy Institute, May 28, 2004.
- [NRC98] “Safety Evaluation by the Office of Nuclear Reactor Regulation Related to NRC Bulletin 96-03, Boiling Water Reactor Owners Group Topical Report NEDO-32686,” U.S. Nuclear Regulatory Commission, August 1998.
- [NRC03] Regulatory Guide 1.82, “Water Sources for Long-Term Recirculation Cooling Following a Loss-of-Coolant Accident,” U.S. Nuclear Regulatory Commission, Office of Nuclear Regulatory Research, Rev. 3, August 2003.
- [URG96] NEDO-32686, Rev. 0, “Utility Resolution Guidance for ECCS Strainer Blockage,” General Electric Nuclear Energy Company, Class 1, November 1996.
- [WEI83] Weigand, G. G. et al., “Two-Phase Jet Loads,” NUREG/CR-2913, Sandia National Laboratory (prepared for the U.S. Nuclear Regulatory Commission), January 1983.
- [HAL80] D. G. HALL, D. G., L. S. CZAPARY, “Tables of Homogeneous Equilibrium Critical Flow Parameters for Water in SI Units,” EG&G Idaho report EGG-2056 (1980).
- [HEN71] HENRY, R. E., FAUSKE, H. K., “The Two Phase Critical Flow of One-Component Mixtures in Nozzles, Orifices, and Short Tubes,” *J. Heat Transfer*, p. 179, May 1971.
- [HAR96] HARVEY, A. H., PESKIN, A. P., KLEIN, S. A., “NIST/ASME Steam Properties: Formulation for General and Scientific Use,” Version 2.11, 1996.
- [WEB76] S. W. Webb, “Evaluation of Subcooled Water Thrust Forces,” *Nucl. Technology* 31, p. 48, October 1976.
- [LAH84] R. T. Lahey and F. J. Moody, *The Thermal-Hydraulics of a Boiling Water Nuclear Reactor*, 3rd ed., La Grande Park, IL: ANS Press, 1984: p. 381.

- [WIT02] Witlox, H. W. and Bowen, P. J., "Flashing Liquid Jets and Two-Phase Dispersion: A Review," United Kingdom Health and Safety Executive Contract Research Report 403/2002, p. 37 (2002).
- [RAH92] Rahn, F.J., Adamantiades, A. G., Kenton, J. E. and Braun, C., *A Guide to Nuclear Power Technology: A Resource for Decision Making*, Krieger, Malabar, Fla., 1992.
- [LOB90] Lobner, P., Donahoe, C. and Cavallin, C., "Overview and Comparison of US Commercial Nuclear Power Plants," prepared for the U.S. Nuclear Regulatory Commission by Science Applications International Corporation, NUREG/CR-5640, SAIC-89/1541, September 1990.

## Attachment 1 to APPENDIX I

```

CCCCCCCCCCCCCCCCCCCCCCCCCCCCCCCCCCCCCCCCCCCCCCCCCCCCCCCCCCCCCCCCCCCC
C           mexFunction C
C MATLAB-executable subroutine that serves as the jumping-off point C
C for calls to the ASME steam tables via the subroutines located in C
C INTPK.FOR and elsewhere. C
C C
C The subroutine MUST be named mexFunction and it MUST contain the C
C four arguments C
C NLHS: number of elements contained in the array PLHS C
C PLHS: an array of pointers to the output values to be returned C
C to MATLAB by mexFunction. It is stored as an array of integer C
C memory references; MATLAB handles extraction of the outputs from C
C these references, but PLHS itself must be populated via the C
C mxCopyReal8ToPtr function (see below). C
C NRHS: number of elements contained in the array PRHS C
C PRHS: array of pointers to input values, as described above for C
C PLHS. The input values themselves are extracted by calling C
C mxCopyPtrToReal8. C
C C
C For this application, the inputs in PRHS and outputs in PLHS are C
C organized as follows: C
C C
C Say that there are y (Po,To,Xo) state points describing a blowdown C
C history. Po(y) [psia] is an array defining the pressures at these C
C points, To(y) [deg F] defines the pressures, and Xo(y) gives the C
C qualities. Only two of these would be specified for each state C
C point; mexFunction will return the third. During the subcooled C
C period, T and P would be given and mexFunction would populate C
C the quality by evaluating  $X = (h - h_f)/h_{fg}$ . Under saturated C
C conditions, either T or P would be given along with X and the model C
C would return the unspecified quantity as  $P = P_{sat}$  or  $T = T_{sat}$ . C
C Other outputs to be returned are C
C C
C Tsat(y) [deg F], saturation temperature C
C Hf(y) [Btu/lbm], enthalpy of liquid phase at Tsat C
C Hg(y) [Btu/lbm], enthalpy of vapor phase at Tsat C
C Rhoo(y) [lbm/ft^3], fluid density C
C Ho(y) [Btu/lbm], fluid enthalpy C
C C
C Note that for saturated fluid there are redundancies, e.g., C
C To=Tsatsat and only three of Hf, Hg, Ho, X are needed. C
C C
C Say that z pressure/temperature contours are to be evaluated. C
C The input would be an array Pj(z) of pressures. The temperatures C
C evaluated for the corresponding y state points would be stored in C
C the array Tj(y*z) indexed by  $Tj[y_i, z_j] = Tj[z*(y_i-1) + z_j]$ . C
C C
C The critical mass flux Ge(y) [lbm/ft^2/s] is computed for each C
C state point, as is the thrust coefficient K (notated TC in the C
C code). This is evaluated using a force balance at the orifice, C
C with the mass flux and thermodynamic state at the orifice being C
C obtained from the model being implemented (the HEM, Henry-Fauske, C
C or the ideal gas law). C
C C
C The pressure Pa(y) and density Rhoa(y) [lbm/ft^3] at the asymptotic C
C plane are also computed. C
C C
C The Ge calculations are carried out using one of three models, C
C homogeneous equilibrium (HEM), Henry-Fauske (H-F), or the ideal gas C
C equations of state. The model used is governed by the value of the C
C USE_LOGIC integer input flag: C
C C
C   USE_LOGIC      Subcooled      Saturated      Superheated C
C   0              HEM             HEM             HEM C
C   1              H-F             H-F             HEM C
C   2              HEM             HEM             Ideal Gas C
C   3              H-F             H-F             Ideal Gas C
C C
C Finally, the saturation temperature Tsat,amb at Pamb is computed, C
C as are the saturated liquid and vapor enthalpies Hf,amb and Hg,amb. C
C C
C The input PRHS is thus C

```

```

C
C CONCAT(Po, To, Xo, Pj, Pamb, y, z, USE_LOGIC)
C
C and the output PLHS is
C
C CONCAT(Po, To, Xo, Tsat, Hf, Hg, Rhoo, Ho, Pa, Rhoa, Ge, TC,
C Tj, Tsat,amb, Hf,amb, Hg,amb) .
C
C AUTHOR: Erich Schneider
C DRAFTED: July 5, 2004
CCCCCCCCCCCCCCCCCCCCCCCCCCCCCCCCCCCCCCCCCCCCCCCCCCCCCCCCCCCC

```

```

SUBROUTINE mexFunction(NLHS, PLHS, NRHS, PRHS)

```

```

C Initialize and dimension other arguments to subroutines located in
C INTPK.FOR. See EXAM.FOR for another example.

```

```

IMPLICIT DOUBLE PRECISION (A-H,O-Z)
INCLUDE 'nprop.cmn'
DIMENSION IWORK(NPROP), IWANT(NPROP), PROPR(NPROP), PROPSI(NPROP)
DIMENSION WAVRI(NRIMAX), RI(NRIMAX), IRIFLG(NRIMAX)
DIMENSION IPCHK(5), IPFLG(5)
INTEGER mxGetM, mxGetN, mxGetPr
INTEGER NLHS, NRHS
INTEGER PLHS(*), PRHS(*)
INTEGER M, N, SIZE, IN_COUNT, OUT_COUNT, IY, IZ, I, J, MODE

```

```

INTEGER IN_PTR, OUT_PTR, USE_LOGIC, USE_MODEL

```

```

C number of outputs per state point. Currently 12: the three inputs
C P, T and X (recall that 2 are specified and this subroutine finds
C the third), Tsat, Hf, Hg, Rhoo, Ho, Pa, Rhoa, Ge, TC
PARAMETER (NUM_OUTPUTS = 12)

```

```

C Dimension input and output arrays given that no more than 50 state
C points and 50 contours may be accepted as inputs.
C This would be a lot more elegant if FORTRAN supported dynamic memory
C allocation, but that's the price one pays for a fast language!
PARAMETER (MAX_STATE_PTS=50, MAX_CONTOURS=50)

```

```

REAL*8 PAMB, TSATAMB, FOFH0, RATIO, MIX_PROP
REAL*8 HFAMB, HGAMB
REAL*8 IN_VALS (MAX_STATE_PTS*3+MAX_CONTOURS+4)
REAL*8 OUT_VALS (MAX_STATE_PTS*NUM_OUTPUTS+
& MAX_STATE_PTS*MAX_CONTOURS+1)
REAL*8 P0 (MAX_STATE_PTS), TO (MAX_STATE_PTS), X0 (MAX_STATE_PTS)
REAL*8 T SAT (MAX_STATE_PTS), HF (MAX_STATE_PTS), HG (MAX_STATE_PTS)
REAL*8 RHO0 (MAX_STATE_PTS), H0 (MAX_STATE_PTS), PA (MAX_STATE_PTS)
REAL*8 RHOA (MAX_STATE_PTS), GE (MAX_STATE_PTS), PJ (MAX_CONTOURS)
REAL*8 TJ (MAX_STATE_PTS,MAX_CONTOURS), TC (MAX_STATE_PTS)

```

```

C Create array of reals from the array PRHS of pointers

```

```

M = mxGetM (PRHS (1))
N = mxGetN (PRHS (1))

SIZE = M*N

IN_PTR=mxGetPr (PRHS (1))

CALL mxCopyPtrToReal8 (IN_PTR, IN_VALS, SIZE)

```

```

C Disassemble and parse input value array: get number of state points
C to be examined and number of P/T contours to be obtained for each
C state point. Note that at least one state point must exist for the
C contour calculation to take place. If this is not the case,
C the contour calculations will be skipped even if Pj input values
C are supplied.

```

```

IY=IN_VALS (SIZE-2)
IZ=IN_VALS (SIZE-1)

```

```

C Obtain value of integer USE_LOGIC flag
USE_LOGIC=IN_VALS (SIZE)

```

```

C Verify that user is not trying to evaluate more than MAX_STATE_PTS
C state points or more than MAX_CONTOURS contours.  If this is the
C case, return a soft landing

      IF (IY .GT. MAX_STATE_PTS) THEN
          CALL mexErrMsgTxt('Number of state points passed to QUERYST is greater
& than MAX_STATE_PTS.  Decrease number of points to be analyzed or
& increase MAX_STATE_PTS in QUERYST.for.')

```

```

      ENDIF
      IF (IZ .GT. MAX_CONTOURS) THEN
          CALL mexErrMsgTxt('Number of contour points passed to QUERYST is great
& er than MAX_CONTOURS.  Decrease number of points to be analyzed or
& increase MAX_CONTOURS in QUERYST.for.')

```

```

      ENDIF

      IN_COUNT=1
      OUT_COUNT=1

C Prepare IWANT vector to harvest enthalpies
```

```

      DO 110 I=1,NPROP
          IWANT(I) = 0
110  CONTINUE
      IWANT(6) = 1
      DO 111 I=1,5
          IPCHK(I) = 0
111  CONTINUE
```

```

C read P_amb and obtain Tsat and enthalpies at P_amb
      PAMB=IN_VALS(SIZE-3)
      CALL TSAT(PAMB, TSATAMB, RHOL, RHOV, IWORK, PROPR, IERR)
```

```

C Compute liquid and vapor enthalpies HF & HG
      CALL PROPS(IWANT, TSATAMB, RHOL, PROPSI, PROPR,0,I2PH,0,
& ISFLG,0, ICFLG, IPCHK, IPFLG, 0, 0, WAVRI, RI, IRIFLG)
      HFAMB = PROPSI(6)

      CALL PROPS(IWANT, TSATAMB, RHOV, PROPSI, PROPR,0,I2PH,0,
& ISFLG,0, ICFLG, IPCHK, IPFLG, 0, 0, WAVRI, RI, IRIFLG)
      HGAMB = PROPSI(6)
```

```

      IF (IY .GT. 0) THEN

C Read (P, T, X) values for IY state points
      DO 100 I=1,IY
          P0(I)=IN_VALS(I)
          T0(I)=IN_VALS(I+IY)
          X0(I)=IN_VALS(I+2*IY)
          GE(I)=0.
          TC(I)=0.
```

```

C Compute properties for this point: first check if fluid is saturated
C QUERYST.FOR treats the fluid as saturated if the input pressure is < 0,
C in which case the input quality should be in [0,1]
```

```

      IF ((P0(I) .LT. 0) .OR. (T0(I) .LT. 0)) THEN
C Saturated conditions with only one of P and T specified; calculate the other
```

```

          IF (P0(I) .LT. 0) THEN
              T_SAT(I) = T0(I)
C Find saturation pressure
              CALL PSAT(T0(I), PMPA, RHOL, RHOV, IWORK, PROPR,
& IERR)
              P0(I) = PMPA
          ELSE IF (T0(I) .LT. 0) THEN
C Find saturation temperature
              CALL TSAT(P0(I), TK, RHOL, RHOV, IWORK, PROPR,
& IERR)
              T0(I) = TK
              T_SAT(I) = T0(I)
          ENDIF
C Find mixture density
          RHO0(I) = MIX_PROP(X0(I), RHOL, RHOV)
```

```

C Compute liquid and vapor enthalpies HF & HG
      CALL PROPS(IWANT, T0(I), RHOL, PROPSI, PROPR,0,I2PH,0,
```

```

&          ISFLG,0, ICFLG, IPCHK, IPFLG, 0, 0, WAVRI, RI, IRIFLG)
          HF(I) = PROPSI(6)

          CALL PROPS(IWANT, T0(I), RHOV, PROPSI, PROPR,0,I2PH,0,
&          ISFLG,0, ICFLG, IPCHK, IPFLG, 0, 0, WAVRI, RI, IRIFLG)
          HG(I) = PROPSI(6)

C Compute mixture enthalpy
          H0(I) = MIX_PROP(X0(I), HF(I), HG(I))

          ELSE

C Find saturation temperature at P0
          CALL TSAT(P0(I), TK, RHOL, RHOV, IWORK, PROPR, IERR)
          T_SAT(I) = TK

C Obtain enthalpies at (Tsat, P0)
          CALL PROPS(IWANT, TK, RHOL, PROPSI, PROPR, 0, I2PH, 0,
&          ISFLG,0, ICFLG, IPCHK, IPFLG, 0, 0, WAVRI, RI, IRIFLG)
          HF(I) = PROPSI(6)
          CALL PROPS(IWANT, TK, RHOV, PROPSI, PROPR, 0, I2PH, 0,
&          ISFLG,0, ICFLG, IPCHK, IPFLG, 0, 0, WAVRI, RI, IRIFLG)
          HG(I) = PROPSI(6)

C Find density and enthalpy at (T0, P0)
          CALL DENS0(DOUT, P0(I),T0(I), DPD, IWORK, PROPR, IERR)
          RHO0(I)=DOUT
          CALL PROPS(IWANT,T0(I),DOUT,PROPSI, PROPR, 0, I2PH, 0,
&          ISFLG,0, ICFLG, IPCHK, IPFLG, 0, 0, WAVRI, RI, IRIFLG)
          H0(I) = PROPSI(6)

          X0(I) = (H0(I) - HF(I))/(HG(I) - HF(I))
          ENDIF

C Given the initial quality, determine the pressure at the asymptotic plane
          IF (X0(I) .GT. -0.1) THEN
              FOFH0 = SQRT(0.1 + X0(I))
          ELSE
              FOFH0 = 0.0
          ENDIF
          RATIO = PAMB/P0(I)
          IF (RATIO .GT. 0.5) THEN
              RATIO=0.5
          ENDIF

          PA(I) = (1. - 1./2.*(1.-2.*RATIO)*FOFH0)*PAMB

C Now find the density. Set MODE = 1 for HSSOLV (Inp: P, H, Out: T, rho)
          MODE = 1
          CALL HSSOLV(MODE, PA(I), H0(I), TPOUT, D1, DV, DL,
&          I2PH, Q, IWORK, PROPR, IERR)

C Format of result in HSSOLV dependent on phase of fluid as signified by I2PH
          IF ((I2PH .EQ. 2) .OR. (I2PH .EQ. 4)) THEN
              RHOA(I) = 1./MIX_PROP(Q, 1.0/DL, 1.0/DV)
          ELSE
              RHOA(I) = D1
          ENDIF

C The code block below sets USE_MODEL based upon user-specified USE_LOGIC
C and upstream stagnation conditions.

C Based upon the specification provided by the user, USE_MODEL is below
C assigned a value of zero (HEM), one (H-F) or two (ideal gas)
C prior to being passed to CRIT_MASS_FLUX. However: if USE_MODEL = 2 and
C upstream stagnation conditions are insufficiently superheated such that
C the ideal gas law yields a static state that is in the two-phase regime,
C CRIT_MASS_FLUX automatically defaults to the HEM. In general, since the
C HEM reduces to the ideal gas law as the superheating increases, USE_LOGIC
C = 2 and 3 should be avoided. This is doubly so since truly ideal gas-like
C behavior is not likely to be observed for any of the problems that are
C being studied with ANSIJET.

          IF (X0(I) .GT. 1.0) THEN
              IF ((USE_LOGIC .EQ. 2) .OR. (USE_LOGIC .EQ. 3)) THEN

```

```

                USE_MODEL = 2
            ELSE
                USE_MODEL = 0
            ENDIF
        ELSE
            IF ((USE_LOGIC .EQ. 0) .OR. (USE_LOGIC .EQ. 2)) THEN
                USE_MODEL = 0
            ELSE
                USE_MODEL = 1
            ENDIF
        ENDIF
        CALL CRIT_MASS_FLUX(GE(I),TC(I),P0(I),H0(I),PAMB,
&                USE_MODEL)
100        CONTINUE
            IN_COUNT=IY*3
                IF (IZ .GT. 0) THEN
C Read Pj values for IZ contours
                DO 101 J=1, IZ
                    PJ(J)=IN_VALS(IN_COUNT+J)
101                CONTINUE
C Compute Tj at each Pj value for every state point
                DO 102 I=1, IY
                    DO 103 J=1, IZ
C MODE = 1 -> HSSOLV expects P and H as inputs and returns T
                        MODE = 1
                        CALL HSSOLV(MODE, PJ(J), H0(I), TPOUT, D1, DV, DL,
&                                I2PH, Q, IWORK, PROPR, IERR)
                            TJ(I,J)=TPOUT
103                        CONTINUE
102                    CONTINUE
                ENDIF
            ENDIF
C Create output array
            DO 104 I=1, IY
                OUT_VALS(I)=P0(I)
                OUT_VALS(I+IY)=T0(I)
                OUT_VALS(I+2*IY)=X0(I)
                OUT_VALS(I+3*IY)=T_SAT(I)
                OUT_VALS(I+4*IY)=HF(I)
                OUT_VALS(I+5*IY)=HG(I)
                OUT_VALS(I+6*IY)=RHO0(I)
                OUT_VALS(I+7*IY)=H0(I)
                OUT_VALS(I+8*IY)=PA(I)
                OUT_VALS(I+9*IY)=RHOA(I)
                OUT_VALS(I+10*IY)=GE(I)
                OUT_VALS(I+11*IY)=TC(I)
                DO 105 J=1, IZ
                    OUT_VALS(NUM_OUTPUTS*IY+(I-1)*IZ+J)=TJ(I,J)
105                CONTINUE
104            CONTINUE
                OUT_VALS(NUM_OUTPUTS*IY+IZ*IY+1)=TSATAMB
                OUT_VALS(NUM_OUTPUTS*IY+IZ*IY+2)=HFAMB
                OUT_VALS(NUM_OUTPUTS*IY+IZ*IY+3)=HGAMB
C Create pointer to output array and size it
                SIZE=MAX_STATE_PTS*NUM_OUTPUTS+MAX_STATE_PTS*MAX_CONTOURS+3
                PLHS(1)=mxCreateDoubleMatrix(SIZE,1,0)
                OUT_PTR=mxGetPr(PLHS(1))
C Populate pointer to output for MATLAB use
                CALL mxCopyReal8ToPtr(OUT_VALS,OUT_PTR,SIZE)
                RETURN
            END
            FUNCTION MIX_PROP(QUALITY, PROP_F, PROP_G)
CCCCCCCCCCCCCCCCCCCCCCCCCCCCCCCCCCCCCCCCCCCCCCCCCCCCCCCCCCCCCCCCCCCC
C                                MIX_PROP                                C

```

```

C Given an input quality and phase properties at saturation, MIX_PROP C
C computes the value of the property for the mixture. Any mass- C
C specific property that has meaning for a two phase mixture C
C (1/density, enthalpy, etc.) may be computed. C
C C
C Inputs: C
C QUALITY Does not necessarily lie in [0,1] C
C PROP_F, PROP_G: saturation values of the property to be computed C
C C
C Output: C
C MIX_PROP = QUALITY*PROP_G + (1-QUALITY)*PROP_F C
C C
CCCCCCCCCCCCCCCCCCCCCCCCCCCCCCCCCCCCCCCCCCCCCCCCCCCCCCCCCCCCCCCC
      REAL*8 QUALITY, PROP_F, PROP_G, MIX_PROP
      MIX_PROP = QUALITY*PROP_G + (1.0-QUALITY)*PROP_F
      RETURN
      END
      SUBROUTINE CRIT_MASS_FLUX(G_CALC, TC_CALC, P0, H0,
& P_AMB, USE_MODEL)
CCCCCCCCCCCCCCCCCCCCCCCCCCCCCCCCCCCCCCCCCCCCCCCCCCCCCCCCCCCCCCCC
C CRIT_MASS_FLUX C
C Given a state point (P0, H0), derives the critical mass flow G C
C (kg/m^2-s) as per the homogeneous equil. method (see Hall & Czapary, C
C "Tables of Homogeneous Equilibrium Critical Flow Parameters for C
C Water In SI Units," EG&G Idaho Report EGG-2056,1980), or the method C
C of Henry and Fauske, "The Two-Phase Critical Flow of One-Component C
C Mixtures in Nozzles, Orifices, and Short Tubes," J. Heat Transfer C
C May 1971, p. 179, or the ideal gas equation of state. C
C C
C HEM Notes C
C C
C The HEM model maximizes the mass flux  $G = V/v$  ( $V$  = flow velocity C
C [m/s],  $v$  = specific volume [m^3/kg]). Applying the First Law, this C
C is equivalent to C
C  $G = 2(h_0 - h)^{1/2} / v$ , C
C where  $h_0$  is the stagnation enthalpy of the fluid, and  $h$  and  $v$  are C
C the enthalpy and specific volume to be adjusted isoentropically C
C such that  $G$  is maximized. The optimum or critical state at which C
C the tradeoff between decreased static enthalpy (and thus higher C
C velocity) and increased specific volume may be represented by a C
C critical pressure,  $p^*$ . It is convenient to optimize on the above C
C using  $p^*$  as the independent variable. C
C C
C The maximization method used is a golden-mean bisection after C
C Teukolsky et. al, "Numerical Recipes in Fortran." The algorithm C
C has been altered somewhat to take into account the nature of the C
C function  $G = f(p^*)$ : since  $f(p^*)$  is undefined for  $p^* > P_0$  and also C
C for very low values of  $p^*$ , some care must be taken in bracketing C
C the root. The algorithm generally converges within 50 iterations, C
C with 1% accuracy being obtained after about 20 evaluations of  $G$ . C
C C
C The algorithm may be tuned by adjusting the fractional tolerance C
C TOLER and the interval size STRETCH_FACTOR over which the root C
C bracketing algorithm searches. C
C C
C Henry-Fauske Notes C
C C
C The Henry-Fauske model also searches for the critical pressure  $p^*$  C
C for which the mass flux is maximized. However, the computational C
C technique is modified somewhat for the Henry-Fauske formulation as C
C it requires solution of a transcendental equation for  $p^*$ . The C
C equation only requires knowledge of upstream stagnation conditions C
C and is described in greater detail in subroutine HENRY_FAUSKE below. C
C C
C To use the same computational engine as that applied to the HEM C
C above, the Henry-Fauske formulation is recast as a maximization C
C problem by writing the transcendental equation for  $p^*$ , C
C  $f(p^*) = g(p^*)$ , C
C in a form amenable to solution via golden-mean maximization: C
C  $A = - (g(p^*) - f(p^*))^2$ , C

```

```

C where the problem becomes one of finding the value of p* that C
C maximizes A, with perfect convergence of course resulting in A = 0. C
C The quantity A is notated P_ROOT in the code below. C
C C
C The same considerations as described for the HEM above apply in C
C connection with root bracketing. Convergence slows for highly C
C subcooled upstream stagnation conditions. Under these conditions, C
C the quantity dG/dp* is very large in the vicinity of the root, and C
C the bracketing of the root becomes an increasingly difficult C
C problem. This is evidenced by the behavior of the equilibrium C
C quality at the throat (notated x_E in Henry and Fauske's paper), C
C which approaches zero for the p* that solves the model as upstream C
C subcooling increases. C
C C
C Ideal Gas Notes C
C C
C Application of the ideal gas equation of state is generally not C
C advisable since the ideal gas approximation is not a good one for C
C upstream stagnation conditions that are only slightly superheated. C
C In fact, it is possible for an evaluation using this method to C
C result in static (choked) conditions that in fact lie within the C
C two-phase regime. If the user has selected ideal gas evaluation C
C and this is found to occur, CRIT_MASS_FLUX defaults to the HEM for C
C G_e and thrust coefficient calculations. Since conditions of C
C interest for ANSIIJET, e.g., main steam line break, are not greatly C
C superheated, it is recommended that users adopt the HEM instead C
C for all superheated evaluations of G_e. C
C C
C The HEM in fact reduces to the ideal gas eqn. for heavily C
C superheated conditions. This provides an additional reason to C
C adopt it. The only disadvantage to the HEM is that the method is C
C somewhat more computationally intensive. C
C C
C C EAS 7/7/04 C
C ***** MODIFICATIONS ***** C
C EAS 7/14/04: Fixed bug that caused code to use improperly C
C initialized values for GE C
C EAS 7/18/04: Deployed Henry-Fauske model solver; added switch to C
C allow user selection of model to use C
C EAS 7/28/04: Fixed root bracketing interval for H-F so that C
C routine will search the entire space of state points C
C allowed by the steam tables. C
C EAS 7/28/04: The model to be used is now an input from the MATLAB C
C function call. See MexFunction for documentation. C
C EAS 7/30/04: Changed to subroutine that computes thrust coeffs. C
C subsequent to critical mass flux calculations C
C EAS 8/17/04 Added ideal gas eqn. of state evaluation C
C C
CCCCCCCCCCCCCCCCCCCCCCCCCCCCCCCCCCCCCCCCCCCCCCCCCCCCCCCCCCCC

```

```

IMPLICIT DOUBLE PRECISION (A-H,O-Z)
INCLUDE 'nprop.cmn'
C Minimum temperature at which steam tables calculate thermo. properties
C Used for bounding of space in which root is to be sought
PARAMETER (T_MIN = 273.2)
DIMENSION IWORK(NPROP), IWANT(NPROP), PROPR(NPROP), PROPSI(NPROP)
DIMENSION WAVRI(NRIMAX), RI(NRIMAX), IRIFLG(NRIMAX)
DIMENSION IPCHK(5), IPFLG(5)
REAL*8 H0,P0,T0,S0,X0,STRETCH_FACTOR,P_HOLD,G_CALC,TC_CALC,R
REAL*8 G_HOLD, MIX_PROP, DENS, VG0, VF0, ROOT_HOLD, P_MIN,RHO_HOLD
REAL*8 T_HOLD
C 0 = HEM, 1 = Henry-Fauske
INTEGER USE_MODEL

C Bracketing triplet p_low=PSTAR(1), p_mid=PSTAR(2), p_hi=PSTAR(3)
C and values of G at each p*
REAL*8 PSTAR(3), GE(3), P_ROOT(3), RHO_T(3)

PARAMETER (GOLD = 1.618034, TOLER=1.0e-5)

C Get temperature T0 and density Rho0 corresponding to (P0, H0)
CALL HSSOLV(1, P0, H0, TPOUT, D1, DV, DL,
& I2PH, Q, IWORK, PROPR, IERR)

```

```

      IF ((I2PH .EQ. 2) .OR. (I2PH .EQ. 4)) THEN
C 2 phase stagnation conditions
      DENS = 1./MIX_PROP(Q, 1.0/DL, 1.0/DV)
      X0=Q
      VF0 = 1./DL
      VG0 = 1./DV
      ELSE IF (I2PH .EQ. -1) THEN
C Saturated / subcooled liquid stagnation
      DENS = D1
      X0= (1./DENS - 1./DL)/(1./DV-1./DL)
      VF0 = 1./DENS
      VG0 = 0.
      ELSE IF (I2PH .EQ. 1) THEN
C Saturated vapor stagnation
      DENS = D1
      X0= (1./DENS - 1./DL)/(1./DV-1./DL)
C Note: although the model functions without crashing for
C superheated vapor, this does not imply its validity!!
      VF0 = 1./DL
      VG0 = 1./DENS
      ENDIF
      T0=TPOUT

C Get entropy S0 corresponding to (T0, Rho0)
      DO 202 I=1,NPROP
      IWANT(I) = 0
202  CONTINUE
      IWANT(7) = 1

      CALL PROPS(IWANT,T0,DENS,PROPSI, PROPR, 1, I2PH, 0,
&ISFLG,0, ICFLG, IPCHK, IPFLG, 0, 0, WAVRI, RI, IRIFLG)
      S0 = PROPSI(7)

      IF (USE_MODEL .EQ. 2) THEN

C Using the ideal gas law for superheated steam:
C T_HOLD and RHO_HOLD will contain the static temperature and density
C at the throat. These are used to verify that the ideal gas law offers
C a reasonably valid model of the expansion.

      T_HOLD = T0
      RHO_HOLD = DENS

      IWANT(8) = 1
      IWANT(9) = 1

C Additional upstream properties are needed:
C Obtain ratio of specific heats, GAMMA = C_P/C_V. GAMMA ~ 1.3 for steam.
111      CALL PROPS(IWANT,T_HOLD,RHO_HOLD,PROPSI, PROPR, 1, I2PH, 0,
& ISFLG,0, ICFLG, IPCHK, IPFLG, 0, 0, WAVRI, RI, IRIFLG)

      IF ((I2PH .EQ. 2) .OR. (I2PH .EQ. 4)) THEN

C If this is true, static conditions at the exit are two-phase. The ideal
C gas equation of state is obviously not applicable. Break and evaluate
C using the HEM.

      USE_MODEL = 0
      GOTO 110
      ENDIF

      GAMMA = PROPSI(9)/PROPSI(8)
C Gas constant R = C_P - C_V [J/kg/K]
      R = 1000.*(PROPSI(9) - PROPSI(8))

C Compute the mass flux noting that P0 is stored in MPa and must be converted
C Hence G_CALC is has units [kg/m^2/s]
      G_CALC = (GAMMA/R*(2./(GAMMA+1.))**((GAMMA+1.)/(GAMMA-1.)))**
& 0.5 * P0 / T0**0.5 *1.e6
C Compute the static discharge density rho = G / V
      RHO_HOLD = G_CALC / (2.*GAMMA*R*T0/(GAMMA+1.))**0.5

C The static pressure at the exit is also needed to compute the thrust coeff:
C This pressure is given in MPa.

```

```

P_HOLD = P0 * (2./(GAMMA+1.))**(GAMMA/(GAMMA-1.))

C Obtain the static temperature, check for consistency, and recompute
C static properties to check validity of ideal gas law eqn. of state:
      T_STAT = T0 * 2./(GAMMA + 1.)
      IF ((T_HOLD - T_STAT)**2. .GT. .01) THEN
          T_HOLD = T_STAT

C Re-evaluate state equation to verify that the correct property values were
C used. If the fluid were behaving as a perfect gas this loop would not be
C necessary. Entropy, for instance, is not conserved between the stagnation and
C static states, although it is approximately constant through the expansion
C for highly superheated conditions.
      GOTO 111
    ENDIF

C Success: the ideal gas law results for G, RHO and P will be used below
C to obtain the thrust coefficient (theoretically 1.26 for steam)

110    ENDIF

      IF(USE_MODEL.EQ. 0) THEN

C Using the HEM:
C Bracket the maximum. It is assumed that Ge(p*) is well-behaved in that
C there will be only one local maximum. Ge(p*=P0) = 0, so we sweep downward
C in p* until we have a triplet (p_low,p_mid,p_hi=P0) in which the root is
C bracketed.

      STRETCH_FACTOR=0.75
      GE(1)=1
      GE(2)=0
      PSTAR(1)=P0

C Increase P* interval to be searched for root until root is bracketed
200    IF (GE(1) .GT. GE(2)) THEN
          PSTAR(1)=PSTAR(1)*STRETCH_FACTOR
          PSTAR(3)=P0
          PSTAR(2)=PSTAR(1)+1./GOLD*(PSTAR(3)-PSTAR(1))
          GE(3)=0.
          CALL EVAL_G(GE(1), RHO_T(1), H0, PSTAR(1), S0)
          CALL EVAL_G(GE(2), RHO_T(2), H0, PSTAR(2), S0)
          IF(GE(2) .LT. TOLER) THEN
C If this is true, we've fallen into an area where both p_low and p_mid
C are undefined. Resize the bracketing interval and try again
          PSTAR(1)=PSTAR(1)/STRETCH_FACTOR
          STRETCH_FACTOR=SQRT(STRETCH_FACTOR)
          GE(1)=GE(2)+TOLER
        ENDIF
        GOTO 200
      ENDIF

201    IF((PSTAR(3)-PSTAR(1))/PSTAR(3) .GT. TOLER) THEN
C Check which interval of (p_low,p_mid), (p_mid,p_hi) is larger and bisect it
      IF(PSTAR(3)-PSTAR(2) .GT. PSTAR(2)-PSTAR(1)) THEN
C The p_mid to p_hi interval is larger; bisect this one
          P_HOLD=PSTAR(3)
          G_HOLD=GE(3)
          RHO_HOLD=RHO_T(3)
          PSTAR(3)=PSTAR(3)-1.0/GOLD*(PSTAR(3)-PSTAR(2))
          CALL EVAL_G(GE(3), RHO_T(3), H0, PSTAR(3), S0)
        ELSE
          P_HOLD=PSTAR(1)
          G_HOLD=GE(1)
          RHO_HOLD=RHO_T(1)
          PSTAR(1)=PSTAR(1)+1.0/GOLD*(PSTAR(2)-PSTAR(1))
          CALL EVAL_G(GE(1), RHO_T(1), H0, PSTAR(1), S0)
        ENDIF
      IF (GE(2) .LT. GE(1)) THEN
C G at p_mid is not at large as G at p_low. Shift bisection interval
C so that old p_mid is now p_hi
          PSTAR(3)=PSTAR(2)
          GE(3)=GE(2)
          RHO_T(3)=RHO_T(2)
          PSTAR(2)=PSTAR(1)

```

```

        GE(2)=GE(1)
        RHO_T(2)=RHO_T(1)
        PSTAR(1)=P_HOLD
        GE(1)=G_HOLD
        RHO_T(1)=RHO_HOLD
    ELSE IF (GE(2) .LT. GE(3)) THEN
C G at p_mid is not at large as G at p_hi. Shift bisection interval
C so that old p_mid is now p_low
        PSTAR(1)=PSTAR(2)
        GE(1)=GE(2)
        RHO_T(1)=RHO_T(2)
        PSTAR(2)=PSTAR(3)
        GE(2)=GE(3)
        RHO_T(2)=RHO_T(3)
        PSTAR(3)=P_HOLD
        GE(3)=G_HOLD
        RHO_T(3)=RHO_HOLD
    ELSE
C bisection interval is fine; continue
    ENDIF
    GOTO 201
ENDIF

C all done, interval size has decreased to specified tolerance.
    G_CALC=GE(2)
    RHO_HOLD=RHO_T(2)
    P_HOLD=PSTAR(2)
    ELSE IF (USE_MODEL .EQ. 1) THEN

C Using Henry - Fauske:
    GE(1)=0
    GE(2)=0
    GE(3)=0
    P_ROOT(1)=-1
    P_ROOT(2)=-1
    P_ROOT(3)=-1

C Bracketing the root and ensuring that the intermediate guess for the
C throat pressure PSTAR results in a larger P_ROOT than the other two
C guesses is a challenge, because the Henry-Fauske evaluation exhibits
C markedly different behavior in the subcooled region as compared to 2-
C phase initial conditions (observe discontinuities in the derivatives
C of the critical mass fluxes shown in Figs 12 through 14 of Henry &
C Fauske). Under subcooled initial conditions, some guesses for throat
C pressure may be invalid as they result in subcooled conditions at the
C throat (see subroutine HENRY_FAUSKE for more). Hence, bracket the root
C by starting with initial bounds of P_low ~ 0, P_high ~ P0. Evaluate
C RHS of 0 = P_ROOT at P_mid, P_low and P_high. If P_ROOT (P_low) is
C closer to zero than at P_mid, try again with P_hi now equal to P_mid.
C If P_ROOT (P_high) is closer to zero than at P_mid, pursue a similar
C strategy by setting P_low = P_hi. Repeat until the P_mid guess gives
C a root evaluation that is closer to zero than either P_low or P_hi.

        PSTAR(3)=P0 - TOLER

C Find the lowest saturation pressure at which steam tables can
C obtain the necessary thermo. properties. This will serve as a
C lower bound for throat pressure derived by the root-finding routine

        CALL PSAT(T_MIN, PMPA, RHOL, RHOV, IWORK, PROPR, IERR)
        PSTAR(1)=PMPA

196        PSTAR(2)=PSTAR(1)+1./GOLD*(PSTAR(3)-PSTAR(1))
        CALL HENRY_FAUSKE(H0, PSTAR(1), T0, S0, X0, P0,
&          VFO, VGO, P_ROOT(1), GE(1), RHO_T(1))
        CALL HENRY_FAUSKE(H0, PSTAR(2), T0, S0, X0, P0,
&          VFO, VGO, P_ROOT(2), GE(2), RHO_T(2))
        CALL HENRY_FAUSKE(H0, PSTAR(3), T0, S0, X0, P0,
&          VFO, VGO, P_ROOT(3), GE(3), RHO_T(3))
        IF (P_ROOT(2) .EQ. 0.0) THEN
            P_ROOT(2)=-1.
            P_ROOT(3)=-1.+TOLER
        ELSE IF (P_ROOT(3) .EQ. 0.0) THEN
            P_ROOT(3)=P_ROOT(2)-TOLER
        ENDIF
        IF (P_ROOT(2) .LT. P_ROOT(1)) THEN

```

```

        PSTAR(3)=PSTAR(2)
        GOTO 196
    ELSE IF (P_ROOT(2) .LT. P_ROOT(3)) THEN
        PSTAR(1)=PSTAR(2)
        GOTO 196
    ENDIF
203     IF ((PSTAR(3)-PSTAR(1))/PSTAR(3) .GT. TOLER) THEN
        IF (PSTAR(3)-PSTAR(2) .GT. PSTAR(2)-PSTAR(1)) THEN
C the p_mid to p_hi interval is larger; bisection this one
            P_HOLD=PSTAR(3)
            G_HOLD=GE(3)
            ROOT_HOLD=P_ROOT(3)
            RHO_HOLD=RHO_T(3)
            PSTAR(3)=PSTAR(3)-1.0/GOLD*(PSTAR(3)-PSTAR(2))
            CALL HENRY_FUSKE(H0, PSTAR(3), T0, S0, X0, P0,
                & VF0, VG0, P_ROOT(3), GE(3), RHO_T(3))
            IF (P_ROOT(3) .EQ. 0.0) THEN
                P_ROOT(3)=P_ROOT(2)-TOLER
            ENDIF
        ELSE
            P_HOLD=PSTAR(1)
            G_HOLD=GE(1)
            ROOT_HOLD=P_ROOT(1)
            RHO_HOLD=RHO_T(1)
            PSTAR(1)=PSTAR(1)+1.0/GOLD*(PSTAR(2)-PSTAR(1))
            CALL HENRY_FUSKE(H0, PSTAR(1), T0, S0, X0, P0,
                & VF0, VG0, P_ROOT(1), GE(1), RHO_T(1))
            IF (P_ROOT(1) .EQ. 0.0) THEN
                P_ROOT(1)=P_ROOT(2)-TOLER
            ENDIF
        ENDIF
        IF (P_ROOT(2) .LT. P_ROOT(1)) THEN
C RHS of 0 = f(PSTAR) as evaluated in HENRY_FUSKE is farther from zero at
C p_mid than at p_low. Shift bisection interval so that old p_mid is now p_hi
            PSTAR(3)=PSTAR(2)
            GE(3)=GE(2)
            P_ROOT(3)=P_ROOT(2)
            RHO_T(3)=RHO_T(2)
            PSTAR(2)=PSTAR(1)
            P_ROOT(2)=P_ROOT(1)
            GE(2)=GE(1)
            RHO_T(2)=RHO_T(1)
            PSTAR(1)=P_HOLD
            GE(1)=G_HOLD
            P_ROOT(1)=ROOT_HOLD
            RHO_T(1)=RHO_HOLD
        ELSE IF (P_ROOT(2) .LT. P_ROOT(3)) THEN
C RHS of 0 = f(PSTAR) as evaluated in HENRY_FUSKE is farther from zero at
C p_mid than at p_hi. Shift bisection interval so that old p_mid is now p_low
            PSTAR(1)=PSTAR(2)
            GE(1)=GE(2)
            P_ROOT(1)=P_ROOT(2)
            RHO_T(1)=RHO_T(2)
            PSTAR(2)=PSTAR(3)
            GE(2)=GE(3)
            P_ROOT(2)=P_ROOT(3)
            RHO_T(2)=RHO_T(3)
            PSTAR(3)=P_HOLD
            GE(3)=G_HOLD
            P_ROOT(3)=ROOT_HOLD
            RHO_T(3)=RHO_HOLD
        ELSE
C bisection interval is fine; continue
        ENDIF
        GOTO 203
    ENDIF
    G_CALC=GE(2)
    RHO_HOLD=RHO_T(2)
    P_HOLD=PSTAR(2)
ENDIF
IF (G_CALC .GT. 0) THEN
    TC_CALC = THRUST_COEFF(G_CALC, RHO_HOLD, P_AMB, P_HOLD, P0)
ELSE
    TC_CALC = 0.
ENDIF

```





```

C Orifice and short tube discharge coefficient as defined on p. 185
C of Henry and Fauske. This fudge factor modifies the critical pressure
C ratio and mass flow rate (see <EQ. 47>). It should be set to unity for
C subcooled flows; for two phase flow, if the flow regime may be considered
C compressible, it may be justified to take a lower value (0.84 is recommended
C in the paper). However, in the interest of conservatism it may be best
C to leave this set to 1.0 throughout.
      ORIFICE_C=1.0
C Define the throat to upstream pressure ratio as per <EQ. 34>
      ETA = PT/P0

C In H-F, liquid phase density at throat equal to upstream stagnation density
C See discussion preceeding and following <EQ. 17>.
      VFT = VF0

C Vapor phase static density at throat (to be computed below if X0 > 0)
      VGT = 0

      DO 310 I=1,NPROP
          IWANT(I) = 0
310  CONTINUE
          IWANT(7) = 1
C Isochoric heat capacity, C_V
          IWANT(8) = 1

      CALL HSSOLV(2, PT, S0, TPOUT, D1, DV, DL,
&              I2PH, Q, IWORK, PROPR, IERR)

      TT = TPOUT
      IF ((I2PH .EQ. 2) .OR. (I2PH .EQ. 4)) THEN
          DENS = 1./MIX_PROP(Q, 1.0/DL, 1.0/DV)
      ELSE
          DENS = D1
      ENDIF

C Saturated liquid and vapor specific volumes at (PT,S0)
      VFE=1./DL
      VGE=1./DV

      CALL PROPS(IWANT,TT,1./VFE,PROPSI, PROPR, 1, I2PH, 0,
&ISFLG,0, ICFLG, IPCHK, IPFLG, 0, 0, WAVRI, RI, IRIFLG)

C Obtain properties of saturated liquid at S0: heat capacity and entropy
      C VF = PROPSI(8)
      SEF = PROPSI(7)

C Approximate pressure derivative of saturated liquid enthalpy by evaluating
C first the change in temperature and liquid density following from a
C change DP in PT with entropy held constant
      CALL HSSOLV(2, PT+DP, S0, TPOUT, D1, DV, DL,
&              I2PH, Q, IWORK, PROPR, IERR)
      PERTURBED_T = TPOUT
C evaluate saturated liquid enthalpy at this new temperature and density
      CALL PROPS(IWANT,PERTURBED_T,DL,PROPSI, PROPR, 1, I2PH, 0,
&ISFLG,0, ICFLG, IPCHK, IPFLG, 0, 0, WAVRI, RI, IRIFLG)

C approximate the derivative by (S(PT+DP)- S(PT))/DP and convert from MPa to Pa
      DSDP = (PROPSI(7)-SEF)/DP*1.e-6

C Obtain entropy of saturated vapor at S0
      CALL PROPS(IWANT,TT,1./VGE,PROPSI, PROPR, 1, I2PH, 0,
& ISFLG,0, ICFLG, IPCHK, IPFLG, 0, 0, WAVRI, RI, IRIFLG)

      SEG = PROPSI(7)

C Write the local equilibrium quality at the throat in terms of phase
C entropies at the throat. Represents quality that fluid would
C possess if phases were allowed to equilibrate <EQ. 23>
      XE = (S0 - SEF)/(SEG - SEF)

C Define the fudge factor correlating dX/dPT to dXE/dPT as per <EQ. 30>
      IF (XE. GT. 0.14) THEN
          N = 1.
      ELSE IF (XE .GT. 0) THEN
          N = XE/0.14
      ELSE

```

```

        N = 0.
    ENDIF

    IF (X0 .GT. 0) THEN
C Isobaric heat capacity, C_p
        IWANT(9) = 1
        I2PH = 2
        FUDGE=0

124         CALL PROPS(IWANT,TT,1./VGE+FUDGE,PROPSI, PROPR, 1, I2PH, 0,
        &             ISFLG,0, ICFLG, IPCHK, IPFLG, 0, 0, WAVRI, RI, IRIFLG)

C This loop is necessary because of apparent fluctuation
C in the least significant digit of the saturated vapor specific volume at P_E,
C VGE. If one calculates this volume using HSSOLV, then feeds it back into PROPS
C to obtain the isobaric heat capacity C_p of the vapor, an error *sometimes*
C results. C_p is not defined for a two-phase mixture; occasionally, the least
C significant digit of VGE varies such that PROPS believes the fluid being passed
C has quality very slightly less than 1.0. C_p, undefined in this regime, is
C returned as zero. Hence, if PROPS indicates that it believes the fluid is 2-phase,
C adjust the density very slightly to return to the vapor-only regime and try the
C calculation again:

        IF(I2PH .EQ. 2) THEN
            FUDGE=FUDGE-(1./VGE)*1.e-8
            GOTO 124
        ENDIF
C Isentropic exponent = C_p/C_V evaluated for saturated vapor at the throat
C (PROPS input arguments are T and sat vapor density at this state point)
        GAMMA = PROPSI(9)/PROPSI(8)
        C_PG=PROPSI(9)
        IWANT(8)=0
        IWANT(9)=0

C Finally, obtain liquid and vapor saturation enthalpies for upstream stagnation
C conditions. Arguments: stagnation temperature and saturated liquid and vapor
C densities
        CALL PROPS(IWANT,T0,1./VG0,PROPSI, PROPR, 1, I2PH, 0,
        &             ISFLG,0, ICFLG, IPCHK, IPFLG, 0, 0, WAVRI, RI, IRIFLG)
        SOG = PROPSI(7)

        CALL PROPS(IWANT,T0,1./VF0,PROPSI, PROPR, 1, I2PH, 0,
        &             ISFLG,0, ICFLG, IPCHK, IPFLG, 0, 0, WAVRI, RI, IRIFLG)
        SOF = PROPSI(7)

C Express the polytropic exponent at the throat. Recall that X_throat = X0 and
C the expansion is isentropic. <EQ. 19>
        POLYTROPIC = ((1.-X0)*C_VF/C_PG + 1)/((1.-X0)*C_VF/C_PG+
        &             1/GAMMA)

C The vapor specific volume at the throat obtained assuming polytropic behavior:
C See <EQS. 18, 19, 38>
        VGT = VG0*(ETA**(-1./GAMMA))

C Collecting terms into ALPHA_0 <EQ. 36>, ALPHA_T <EQ. 37> and BETA <EQ. 38>:
        ALPHA_0 = X0*VG0/((1.-X0)*VF0+X0*VG0)
        ALPHA_T = X0*VGT/((1.-X0)*VF0+X0*VGT)

        BETA = (1./POLYTROPIC+(1.-VF0/VGT))*((1.-X0)*N*PT*1.e6*DSDP/
        &             (X0*(SEG-SEF)))-C_PG*(1./POLYTROPIC-1./GAMMA)/(SOG-SOF)

C Compute the RHS of <EQ. 33>
        GG = GAMMA/(GAMMA-1.)
        RHS = (((1.-ALPHA_0)*(1.-ETA)/ALPHA_0+GG)/
        &             (1./(2.*BETA*ORIFICE_C*ORIFICE_C*
        &             ALPHA_T*ALPHA_T)+GG))**(GG)

C To make this amenable to numerical solution via maximization, return the
C value -(RHS-ETA)^2, which will exhibit a maximum value of zero when the
C correct guess for the root, PT, is supplied.
        RHS = RHS-ETA
        ROOT=- (RHS*RHS)

C At last, evaluate the critical mass flux as a function of PT
        GCRT=(X0*VGT/(POLYTROPIC*PT*1.e6)+(VGT-VF0)*((1.-X0)*N/(SEG-
        &             SEF))*DSDP-(X0*C_PG*(1./POLYTROPIC-1./GAMMA)/(PT*1.e6*

```

```

&      (SOG-S0F))))**(-0.5)
      ELSE
C Subcooled upstream stagnation conditions
      IF (XE. GT. 0) THEN
C Pressure ratio guess was valid in that quality at the nozzle is nonzero
      GCRIT=((VGE-VF0)*N*DSDP/(SEG-SEF))**(-0.5)
      RHS = 1. - VF0*GCRIT*GCRIT/2/(P0*1.e6)/ORIFICE_C/ORIFICE_C
      RHS = RHS-ETA
      ROOT = -(RHS*RHS)
      ELSE
C Pressure ratio guess was not good, resulting in subcooled nozzle conditions.
C H-F does not function under these conditions -- see <EQ. 45> w/ N = 0.
C Return zero mass flux so that the root finder knows to discard this attempt.
      GCRIT = 0
      ENDIF
    ENDIF
C Return the fluid density at the throat to CRIT_MASS_FLUX for use in calculating
C the thrust coefficient. Specifying the mass flux and fluid density also
C specifies the velocity of the homogenized fluid.
    IF (GCRIT .GT. 0) THEN
      IF (X0. LE. 0) THEN
        RHO_T = 1./VFT
      ELSE IF (X0 .LE. 1) THEN
        RHO_T = 1./MIX_PROP(X0,VFT,VGT)
      ELSE
        RHO_T = 1./VGT
      ENDIF
    ELSE
      RHO_T = 0
    ENDIF
  END
  FUNCTION THRUST_COEFF(GE, RHO_T, P_AMB, PT, P0)
CCCCCCCCCCCCCCCCCCCCCCCCCCCCCCCCCCCCCCCCCCCCCCCCCCCCCCCCCCCCCCCCCCCC
C      THRUST_COEFF C
C Calculates the thrust coefficient by C
C C
C      K = PT/P0*(1+G^2/RHO_T/PT), C
C where C
C P0 and PT are the stagnation and throat pressures [Pa_gauge] C
C G is the mass flux [kg/m^2/s] as evaluated by H-F or the HEM, C
C RHO_T is the fluid density [kg/m^3] at the throat C
C EAS 7/30/04 C
CCCCCCCCCCCCCCCCCCCCCCCCCCCCCCCCCCCCCCCCCCCCCCCCCCCCCCCCCCCCCCCCCCCC
      REAL*8 GE, RHO_T, P_AMB, PT, P0, THRUST_COEFF
      THRUST_COEFF=(PT-P_AMB)/(P0-P_AMB)*(1.0+GE*GE/
& RHO_T/((PT-P_AMB)*1.e6))
      RETURN
      END

```

```

function [p,t,x,ts,hf,hg,d,h0,pa,da,ge,tc,tj,ta,hfa,hga] = ...
    GetProperties(pres, temp, qual, pdmg, pamb, use_model)

% Given N (pres, temp, qual) state points and M damage
% pressures, GetProperties invokes the NIST steam tables
% to obtain
% p[N] state point pressures    [psi]
% t[N] temperatures            [deg F]
% x[N] qualities                [-]
% ts[N] saturation temperatures [deg F]
% hf[N] liquid phase enthalpies at ts [Btu/lbm]
% hg[N] vapor phase enthalpies at ts [Btu/lbm]
% d[N] densities                [lbm/ft^3]
% h0[N] enthalpies             [Btu/lbm]
% pa[N] pressures at asymptotic plane [psi]
% da[N] densities at asymptotic plane [lbm/ft^3]
% ge[N] critical mass fluxes    [lbm/ft^2/s]
% tc[N] thrust coefficients     [-]
% tj[N][M] temperatures at pdmg[M] [deg F]
% ta saturation temp at ambient pres. [deg F]
% hfa liquid phase enthalpy at ta [Btu/lbm]
% hga vapor phase enthalpy at ta [Btu/lbm]
%
% EAS 7/12/04
%
% 7/28/04:
% To obtain the ge and tc, GetProperties uses the HEM or H-F according to
% the rule specified by the integer flag use_model. See ansijet.m and
% QUERYST.FOR for documentation regarding use_model.

n_outputs=12;

% define conversion factors for use in UnitConverter
pres_conv = [0 0 0 0 1 0];
temp_conv = [1 0 0 0 0 0];
enth_conv = [0 -1 0 1 0 0];
dens_conv = [0 1 -3 0 0 0];
mflx_conv = [0 1 -2 0 0 0];

% convert from english to SI units
pres=UnitConverter(pres,pres_conv);
temp=UnitConverter(temp,temp_conv);
pdmg=UnitConverter(pdmg,pres_conv);
pamb=UnitConverter(pamb,pres_conv);

% concatenate inputs. This is not strictly necessary
% since the mex routine can handle multiple input variables,
% but the functionality would be identical regardless
% the last two inputs should be the number of state points
% and the number of contours per state point

npts=size(pres);
npts=npts(:,2);

nconts=size(pdmg);
nconts=nconts(:,2);

mex_input=[pres temp qual pdmg pamb npts nconts use_model];

% call QUERYST.FOR via QUERYST.DLL
mex_output=queryrst(mex_input);

% reconstruct outputs
for i=1 : npts
    p(i)=mex_output(i);
    t(i)=mex_output(i+npts);
    x(i)=mex_output(i+npts*2);
    ts(i)=mex_output(i+npts*3);
    hf(i)=mex_output(i+npts*4);

```

```

hg(i)=mex_output(i+npts*5);
d(i)=mex_output(i+npts*6);
h0(i)=mex_output(i+npts*7);
pa(i)=mex_output(i+npts*8);
da(i)=mex_output(i+npts*9);
ge(i)=mex_output(i+npts*10);
tc(i)=mex_output(i+npts*11);
for j=1 : nconts
    tj(i,j)=mex_output(npts*n_outputs+(i-1)*nconts+j);
end
end
ta=mex_output(npts*n_outputs+npts*nconts+1);
hfa=mex_output(npts*n_outputs+npts*nconts+2);
hga=mex_output(npts*n_outputs+npts*nconts+3);

% if no pressure / temperature contours were requested, create an empty
% dummy tj to avoid undefined variable contours later on
if(nconts==0)
    tj=[];
end

% convert back from SI to english units
p=UnitConverter(p,-pres_conv);
t=UnitConverter(t,-temp_conv);
ts=UnitConverter(ts,-temp_conv);
hf=UnitConverter(hf,-enth_conv);
hg=UnitConverter(hg,-enth_conv);
h0=UnitConverter(h0,-enth_conv);
pa=UnitConverter(pa,-pres_conv);
d=UnitConverter(d,-dens_conv);
da=UnitConverter(da,-dens_conv);
ge=UnitConverter(ge,-mflx_conv);
ta=UnitConverter(ta,-temp_conv);
tj=UnitConverter(tj,-temp_conv);
hga=UnitConverter(hga,-enth_conv);
hfa=UnitConverter(hfa,-enth_conv);
return

```

```

function conv_x = UnitConverter(x_o, dimension_array)

conv_factors = zeros(size(dimension_array));

% converts a quantity from the english unit system to SI
% or vice versa, returning the converted value as conv_x.
% x_o quantity (in english or SI units) to be converted
% default operation is english -> SI
% dimension_array of integers describing the english system
% unit to be converted to SI, viz:

% (1) temperature conversion F -> K
conv_factors(1)=5./9.;
% (1) can only take on the values 1 (F->K) and -1 (K->F).
% If (1) is nonzero, all other members of dimension_array
% will be ignored!
% (2) lbm -> kg
conv_factors(2)=0.45359237;
% (3) ft -> m
conv_factors(3)=0.3048;
% (4) Btu -> kJ
conv_factors(4)=1.05505585;
% (5) psi -> MPa
conv_factors(5)=0.00689475729;
% (6) deg F -> deg K
conv_factors(6)=5./9.;
%
% The value passed is the exponent of the unit to be converted.
% Example usage: to convert density [lbm/ft^3] to SI units,
% one would pass dimension_array = [0 1 -3 0 0 0].
% To convert [kg/m^3] back to [lbm/ft^3], one would simply
% obtain the inverse of the conversion factor applied previously
% by passing [0 -1 3 0 0 0].

result = x_o;
if dimension_array(1) == 1
    result = (result + 459.4) * conv_factors(1);
elseif dimension_array(1) == -1
    result = result / conv_factors(1) - 459.4;
else
    for i = 2:length(conv_factors)
        if dimension_array(i) ~= 0
            result = result * conv_factors(i)^dimension_array(i);
        end
    end
end
conv_x = result;

```